Production and Dynamic Mechanical Analysis of Macro-Scale Functionalized Polydicyclopentadiene Objects Facilitated by Rational Synthesis and Reaction Injection Molding

Tyler J. Cuthbert, Tong Li, and Jeremy E. Wulff

2019

Production and Dynamic Mechanical Analysis of Macro-Scale Functionalized Polydicyclopentadiene Objects Facilitated by Rational Synthesis and Reaction Injection Molding

Tyler J. Cuthbert, [†] *Tong Li,* [†] *and Jeremy E. Wulff**

Department of Chemistry, University of Victoria, PO Box 3065 STN CSC, Victoria, British Columbia, V8W 3V6, Canada.

KEYWORDS: functionalized polymers, polydicyclopentadiene, reaction injection molding, dynamic mechanical analysis, structure-property relationships

ABSTRACT: Polydicyclopentadiene (PDCPD) is a ring-opening metathesis polymer derived from dicyclopentadiene. Valued for its light weight, excellent material strength, and good performance at both high and low temperatures, PDCPD is used to make body panels for tractors and heavy-duty trucks. We recently described the first functionalized form of PDCPD (*f*PDCPD) that maintains the thermal stability of the parent polymer. However, while commercial PDCPD components are produced through a reaction injection molding process on very large scale, our *f*PDCPD polymer was developed on small scale, and has not been shown to be a viable substrate for reaction injection molding processes. Here we address these limitations by providing an improved synthesis of the *f*DCPD monomer mixture on half-kilo scale, and describing a method for separating the polymerizeable monomer from other, nonpolymerizeable, regioisomers without chromatography. We further demonstrate a reaction injection molding process for the creation of prototype *f*PDCPD components. Together, these increases in scale and advances in small object manufacturing facilitate the production of regular-dimensioned samples for dynamic mechanical analysis, permitting the first direct comparison of the mechanical properties of *C*-linked ester-functionalized PDCPD with those of unmodified PDCPD. Additionally, by employing monomers of different regioisomer purity, products are achieved encompassing a broad range of glass transition temperatures and storage/loss moduli.

INTRODUCTION

Incorporation of functional groups into the structure of known polymer materials can provide a means to improve certain desirable properties while maintaining the best features of the existing polymer. At the same time, however, this strategy carries an additional synthetic burden in that the functionalized monomers required for polymerization will themselves need to be made on large scale. For example, while polyvinylchloride (PVC) has certain material advantages over polyethylene that make it the world's third-most widely produced synthetic polymer[1,2] (despite toxicity concerns[3,4,5]), the efficient synthesis of the vinyl chloride monomer remains a substantial challenge.[6,7] Currently about 85% of vinyl chloride is produced through a rather complicated process in which ethylene is first chlorinated to yield 1,2-dichloroethane, which is then thermally cracked to produce the desired vinyl chloride monomer together with an equivalent of HCl.[7,8] The HCl is then reacted with more ethylene in a copper-catalyzed oxychlorination process that generates additional 1,2-dichloroethane for cracking to afford still more of the desired monomer. It is apparent, then, that even for industrially important bulk materials like PVC for which annual worldwide production exceeds 10 billion kilograms each year, synthesis of a functionalized monomer can require considerable attention.

Polydicyclopentadiene (PDCPD) is an example of an industrially important material that could benefit from the incorporation of additional functionality. Produced through ring-opening metathesis polymerization (ROMP) of dicyclopentadiene (DCPD), PDCPD's extensive network of chemical crosslinks provides an extremely high material strength without contributing to excessive brittleness.[9,10] These properties are maintained at both low temperatures and high temperatures.[11,12,13] After initially being employed to make cowlings for snowmobiles, PDCPD is now used to make body panels, bumpers, and other components for tractors and commercial

trucks.[11] Importantly, these commercial products are made using a reaction injection molding process in which the polymerization and crosslinking reactions happen together within the mold to generate the final product.[11,14,15,16,17] Spent catalyst remains trapped within the material.

Although useful for many applications, PDCPD has several disadvantages that may be traced back to its lack of functionality. These include a low surface energy when freshly prepared (which makes it difficult to attach PDCPD parts to other objects using conventional adhesives, without first employing a surface oxidation process),[18] a lack of chemical tunability (due to the absence of any functionality other than C–C or C–H bonds), an unpleasant odor (due to residual DCPD being trapped within the final product and then slowly released to the environment)[19,20,21] and a lack of recyclability (since the bonds formed in the crosslinking steps cannot be undone, as is true of most thermoset polymers).[22] Introduction of a functional group could mitigate many of these disadvantages. While several methods are known to result in functionalization of the residual C=C double bonds within the polymer structure (i.e. *post*-polymerization functionalization),[23,24,25,26] very few options are available for functionalization of the DCPD monomer in such a way that the functional group does not impede polymerization and can be carried through into the polymer product (i.e. *pre*-polymerization functionalization).[21,27]

We rationally designed a *functionalized* form of polydicyclopentadiene (*f*PDCPD, Figure 1), in which an ester group was incorporated at the unstrained olefin within the dicyclopentadiene monomer.[28,29] This material undergoes polymerization and thermal crosslinking similarly to traditional DCPD, with the exception that the two steps can now be done separately. If desired, linear *f*PDCD can easily be isolated and purified prior to the crosslinking event. Although synthesis of linear unfunctionalized PDCPD has been reported by other groups, it is generally more challenging to achieve.[30,31,32,33,34]

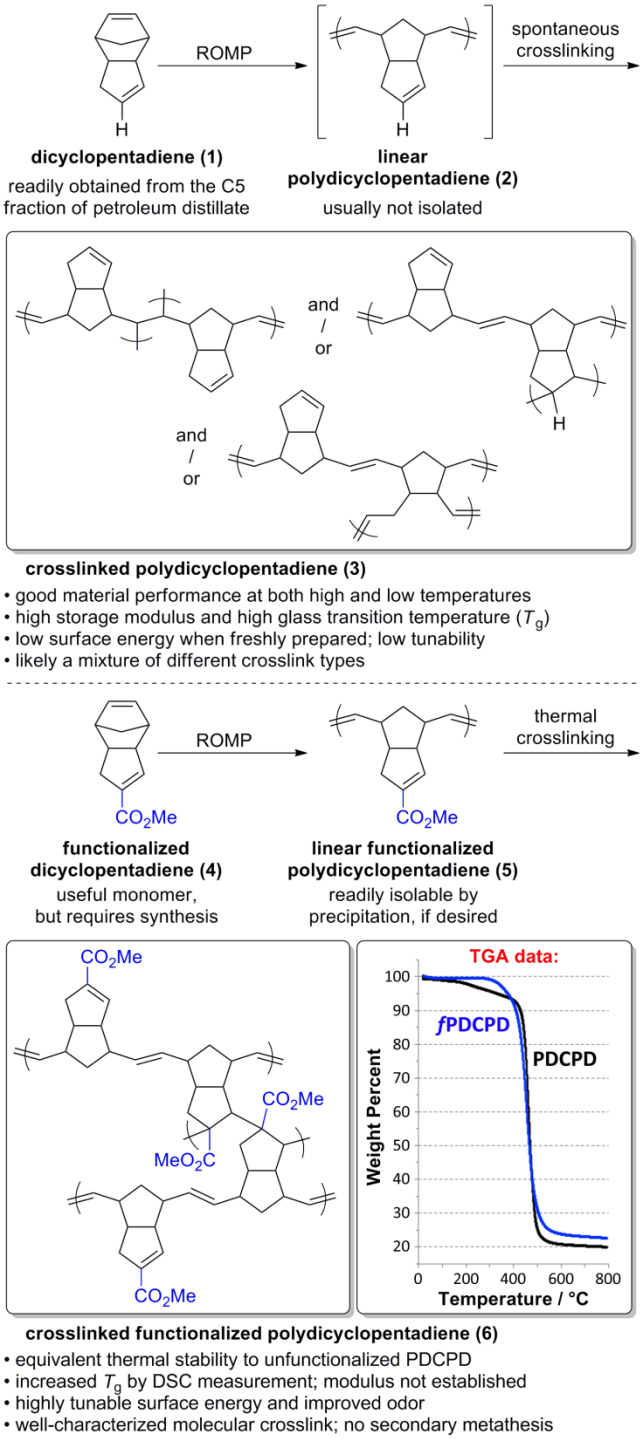

Figure 1. Comparison of traditional PDCPD to *f*PDCPD. Inset shows thermogravimetric analysis for synthesized, crosslinked *f*PDCPD polymer vs. commercial unfunctionalized PDCPD (Product Rescue BVBA).

The incorporation of the ester functional group within our *f*PDCPD confers several advantages – the surface energy of the final product can now be readily tuned through (fractional) saponification, and the monomer itself has a more pleasant smell owing to the presence of the ester.[28] Moreover, while the exact structure of the chemical crosslinks within traditional PDCPD has been a matter of considerable debate,[35,36] the presence of the ester group reduces the number of reasonable crosslinking reactions. In parallel work, we showed that the structure of the crosslink in our *f*PDCPD is predominantly that shown in Figure 1, in which the critical C–C bond forms through a head–tail linkage of the embedded methyl methacrylate motif.[29] This (at least in principle) provides a means for chemically reversing the thermally formed chemical crosslink, which could in turn form the basis of a recycling process. Critically, the incorporation of the ester functional group does not detract from the desirable properties of PDCPD – in contrast to other known types of functionalized polydicyclopentadiene (wherein the functional group is attached through a labile allylic ester linkage),[21,27] our *C*-linked ester-functionalized polymer maintains PDCPD's high glass transition temperature, and shows a similar resistance to decomposition at high temperatures.[28,29]

At the same time, our approach begets additional synthetic challenges. Whereas dicyclopentadiene itself is readily available from petrochemical stocks,[37,38] our monomer (**4**) requires the investment of synthetic effort to attach the ester group. Although an efficient method for the production of **4** was developed based upon our earlier Thiele's ester research (Figure S1),[39] this method unfortunately does not afford **4** as the sole regioisomer. Instead, a mixture of regioisomers is generated, in which **4** is only the second-most abundant species.

We previously showed that flash-column chromatography could be used to isolate a mixture of **4** and its principal regioisomer, **9**. While the ratio of **4**:**9** was unfortunately not tunable

through the addition of Lewis acids or other additives, we found that monomer **4** could be selectively polymerized from this mixture to afford the desired linear *f*PDCPD polymer, which could in turn be subjected to thermal crosslinking. Although the protocol efficiently provided both linear and crosslinked polymer for study, it was deemed insufficient for scale-up to production quantities, because of the following reasons:

(1) Separation of the mixture of **4** and **9** from other species employed a chromatographic separation, which would be costly on large scale;

(2) Selective polymerization of **4** from the monomer mixture necessitated the separation of the resulting polymer (**5**) from unreacted **9**; this was typically accomplished through centrifugation, which would be prohibitively expensive on large scale;

(3) Polymerization from a monomer mixture would be incompatible with reaction injection molding, which is the dominant technique employed for the commercial production of PDCPD automotive parts;

(4) The synthesis and polymer precipitation made use of flammable solvents, which would be undesirable in an industrial setting;

(5) In our initial work, high catalyst loadings were reported (40:1 substrate:catalyst), which would increase the cost of the final product since the metathesis catalyst used for this work (Grubbs 2nd generation catalyst) is relatively expensive;

(6) Although the mixture of **4** and **9** was prepared on reasonable scale (up to 45 grams), only milligram-quantities of polymer were synthesized initially, raising questions about how scalable the polymerization would be.

In this report, we address all of the above challenges and also demonstrate a proof-of-concept reaction injecting molding process for *f*PDCPD. These advances permit the creation of macro-scale *f*PDCPD objects suitable for more advanced materials testing.

RESULTS AND DISCUSSION

Large-Scale Production of *f*DCPD Monomer. We began our study by seeking to increase the scale of our initially-developed route to the linear *f*PDCPD polymer, while minimizing the use of flammable solvents (especially the diethyl ether used previously for polymer precipitation) and avoiding the use of chromatography for the isolation of the **4**:**9** mixture. This necessitated a more thorough assessment of the various species formed through the Diels–Alder reaction of carboxylated cyclopentadiene (i.e. the protonated form of **8**) with cyclopentadiene itself.

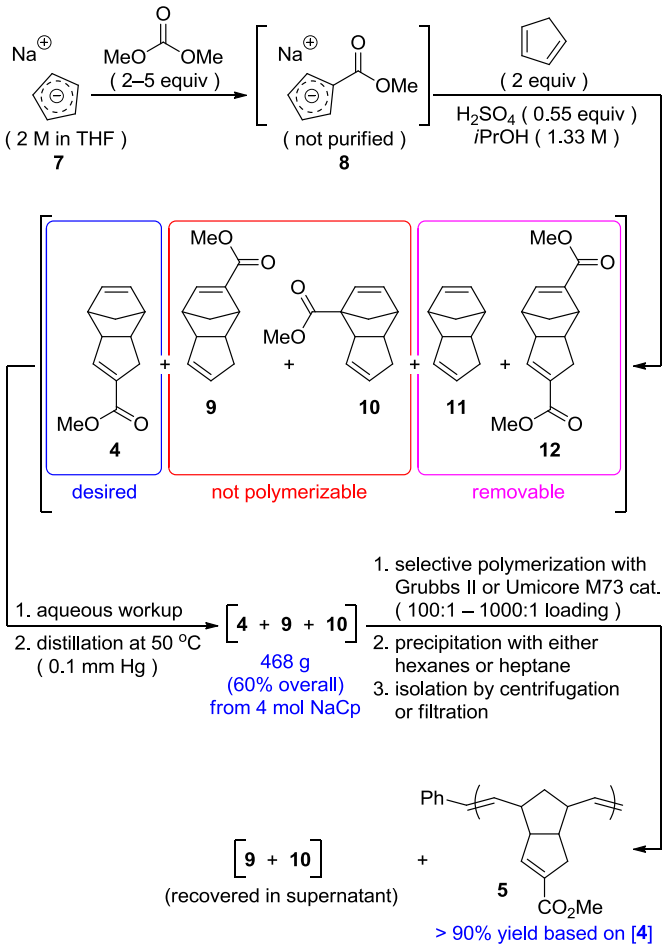

Figure 2. Improved conditions for producing *f*DCPD and *f*PDCPD on large scale. Compounds **4**, **9**, **10**, **11** and **12** are all produced as *endo* Diels–Alder adducts.

As shown in Figure 2 (and presented in more detail in the Supporting Information), extensive spectroscopic analysis revealed the presence of the four species that had been described previously (heterodimers **4** and **9**, together with homodimers **11** and **12**),[28] along with one additional minor regioisomer (**10**) visible in the crude NMR spectrum. The connectivity of the newly identified regioisomer – which is consistent with our earlier mechanistic predictions[40,41] (see Figure S2) – establishes within the molecule a strained norbornyl C=C double bond without any additional substituents. We were therefore concerned that **10** might

participate in the polymerization reaction alongside **4** or, worse yet, react non-productively with the ruthenium catalyst to shut down the reaction. Fortunately, a series of polymerization trials with mixtures of **4**, **9**, **10** and **12** in various states of purity showed **10** to be a harmless spectator under our standard polymerization conditions (room temperature reactions using Grubbs 2nd generation catalyst). We found that selective polymerization proceeded efficiently so long as the more-reactive dicyclopentadiene (**11**, formed from the excess cyclopentadiene used in the Diels–Alder step) was removed first (*vide infra*), and provided that only hexane-soluble material was used for the reaction.[42]

The critical observation that isomer **4** could be selectively polymerized out of even more complex mixtures than had been envisaged in our earlier work set the stage for the eventual large scale monomer synthesis described in Figure 2. Turning our attention first to the carbonylation of sodium cyclopentadienylide (NaCp; **7**) to provide **8**, we found that we could reduce the amount of dimethyl carbonate from 5 equivalents down to 2 equivalents without any significant loss in yield. Perhaps more importantly, we found that even on large scale no additional solvent was required for the carbonylation step; we merely used the THF that the initial NaCp reagent was prepared in.[43] Kilo-scale production of polymer would most likely start from commercially sourced NaCp in THF (e.g. Boulder Scientific sells NaCp as a 20 wt% solution in THF/toluene, in 85-kg cylinders).

In previous work aimed at the synthesis of Thiele's esters, we showed that sodium salt **8** could be purified by washing with diethyl ether.[39] However, in the interest of minimizing the use of flammable solvent, we omitted this step here. Instead, volatile materials (THF and dimethylcarbonate) were simply removed from **8** through rotary evaporation, and the residue was combined with dicyclopentadiene, isopropanol, and 0.55 equivalents of sulfuric acid to promote

the controlled re-protonation of the substrate, followed by heterodimerization. Stirring for 48 hours produced the mixture of dicyclopentadienes shown in Figure 2, in which key intermediate **4** was typically present as about 15–20% of the total mixture. A simple aqueous workup using hexanes and water was sufficient to remove inorganic byproducts, along with other impurities that were found in control experiments to cause problems for the upcoming polymerization step. Although it was not necessary to remove **12** (since it does not readily participate in metathesis polymerization), its lower solubility in hexanes relative to the other species in the reaction mixture meant that it was also mostly excluded at this stage.

The use of 2 equivalents of dicyclopentadiene in the Diels–Alder reaction is necessary to favor the formation of heterodimer **4** over the competing production of Thiele's ester **12**. The excess dicyclopentadiene, however, necessarily leads to the production of homodimeric unsubstituted dicyclopentadiene (**11**) by the end of the reaction period. This can be recycled, provided that it can be efficiently removed from the reaction mixture. Indeed, it is vital to do so, since it would otherwise participate in the polymerization reaction. While copolymers of **11** and **4** are undoubtedly interesting (and are being pursued by us in other work) they are not the focus of our current scale-up efforts.

After considerable experimentation, we found that gentle distillation at 50 °C and 0.1 mm Hg was sufficient to remove the unwanted dicyclopentadiene from the reaction mixture.[44] Recovered dicyclopentadiene is reasonably pure (see Figure S3 in the Supporting Information) and can therefore be cracked and reused in the Diels–Alder step.

By following the optimized protocol described above, we were able to carry through material on up to a 4 mol scale, to achieve a yield of 468 g (60%, based upon the amount of NaH

used to prepare the starting material, **7**) of monomer mixture (containing crude **4** (30%), **9** (57%) and **10** (13%)) in a single batch. Only standard laboratory glassware and rotary evaporators were employed, and no chromatography was used throughout the process. This represents a substantial improvement over our earlier synthetic route.

Selective Polymerization of 4 From Crude Monomer Mixture. Because monomer **4** appeared to be the only species within the crude mixture that could be polymerized with the Grubbs 2nd generation catalyst at room temperature, we investigated the production of *f*PDCPD through selective polymerization of the crude material.

We found that polymerization from the unpurified **4**:**9**:**10** mixture afforded linear polymer (**5**) that was spectroscopically identical to that prepared from the column-purified **4**:**9** mixture used for our earlier studies (Figure 3). No incorporation of any other monomer could be identified.

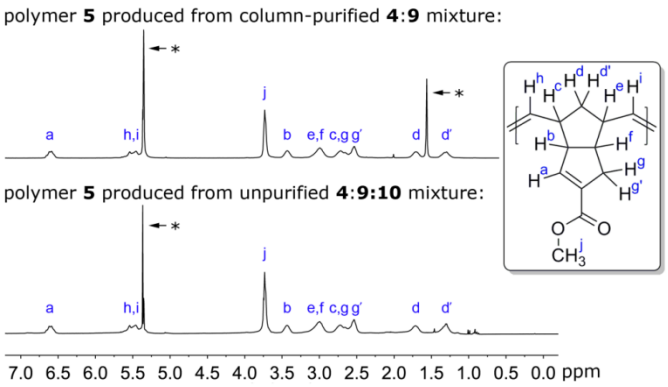

Figure 3. Representative ^{1}H NMR spectra for linear *f*PDCPD polymer prepared from original column-purified monomer[28] mixture vs. that prepared from the unpurified mixture of regioisomers described here. Signals labeled with asterisks indicate CH_2Cl_2 and H_2O in the CD_2Cl_2 NMR solvent. See Figures S16 and S17 for ^{13}C NMR assignments for the linear polymer, and reference 29 for solid-state ^{13}C spectra of the crosslinked material.

Improvements to Catalyst Loading. We next explored the effect of different catalyst loadings upon both column-purified and unpurified monomer mixtures. In both cases, we observed efficient polymerization reactions with loadings as low as 1000:1 substrate:catalyst – a significant improvement over our initial results.[45] Recognizing that the use of Grubbs 2nd generation catalyst could become problematic on very large scale (the original Grubbs catalysts are rather carefully controlled by Materia, and are expensive for production scale reactions), we also explored the use of the competing Umicore M73 catalyst for which we were quoted a much more competitive price for large quantities. As expected, the Umicore catalyst was also effective at promoting the polymerization of **4** (at a 100:1 substrate:catalyst loading),[45] even from within impure mixtures. For all of these polymerization experiments it was difficult to determine exact rates because with low catalyst loadings the molecular weight of the resulting linear polymer becomes large and solubility is compromised, which complicates NMR analysis (see Table S1 and Figure S18). Suffice it to say, however, that selective polymerization of **4** remained robust for both catalysts across a variety of loadings and starting material purities.

Alternative Purification Strategies for Linear Polymer 5. In our initial research, linear *f*PDCPD **5** was precipitated with diethyl ether and collected by centrifugation prior to thermal curing. Both the solvent and the collection method were therefore problematic from the perspective of scale up. We evaluated the use of other solvents for the precipitation step, and found that both hexanes and heptane (a less-flammable and less-toxic solvent that is often used as a process-chemistry replacement for hexanes)[46,47,48,49] were effective in precipitating polymer **5** from the mother liquor with no loss in yield.

Filtration was also briefly explored as an alternative to centrifugation. While this facilitated isolation of the linear polymer, benchtop filtration conditions necessarily exposed the product to

more air than centrifugation or decanting of the supernatant. It is well known that polydicyclopentadiene is somewhat prone to aerobic oxidation,[26,50,51] and we have shown previously that **5** undergoes slow oxidative crosslinking when allowed to stand in air.[28] The resulting poor solubility for batches of **5** isolated by filtration led us to abandon this method in favor of simply decanting the supernatant containing the unreactive monomers, in cases where centrifugation was impractical.

Development of a Reaction Injection Molding Process for *f*PDCPD. Our efforts so far had greatly improved access to the functionalized dicyclopentadiene monomer **4** in a form that was useful for polymerization, but at this stage the polymer itself still had to be separated from unreacted **9** (as well as smaller amounts of **10**) in a tedious centrifugation or decanting step. Moreover, the linear polymer **5** was difficult to form into solid objects suitable for advanced materials testing. In preliminary experiments using a Carver press, we were able to compress **5** into uneven disks that could be thermally cured either in the press or in a separate operation – but objects prepared in this way suffered from defects and voids throughout their macroscopic structure that would have complicated rheology or other measurements. In addition, the use of linear polymer **5** in injection molding operations would require high pressures to flow the polymer into a mold, since the temperature would have to be maintained below the crosslinking onset temperature (*ca.* 135 °C). For any current industrial process designed around the well-developed reaction injection molding of traditional polydicyclopentadiene to switch over to the use of prepolymer **5** would require a substantial retooling effort that may not be warranted for such an untested material. In order to gain more rapid acceptance of our technology with current users of polydicyclopentadiene, we reasoned that a method where monomer **4** could be directly subjected to reaction injection molding was therefore desirable.

We briefly studied the polymerization of the crude **4**:**9**:**10** mixture described above, in the absence of solvent. As expected, the selective polymerization proceeded smoothly, but objects prepared in this way were very soft, and easily deformable (see below for further discussion of this material, and accompanying modulus data). Presumably the large amounts of unreacted **9** and **10** that are necessarily incorporated into the final polymer act as plasticizers. In order to develop an efficient injection molding process, we clearly required access to a form of monomer **4** that was relatively free of these contaminating species.

We had already shown that chromatographic separation of **4** and **9** was extremely difficult (although the two compounds are fairly easy to separate from other isomers including **10**, they are challenging to separate from one another) – and in any case we hoped to minimize the use of chromatography throughout our processes. Attempted fractional distillation was likewise unsuccessful. We therefore elected to take advantage of the very different reactivity of **4** and **9** toward nucleophiles. It was well known that the strained α,ß-unsaturated ester in **9** was much more electrophilic than the unstrained α,ß-unsaturated ester in **4**.[52] Indeed, we[28] and others[52] had previously taken advantage of this difference to purify **4** for characterization purposes. We now sought to test whether a selective conjugate addition could be employed to separate **4** from **9** on preparative scale.

We elected to use 1,3-diaminopropane (**13**) as the nucleophile in this reaction, reasoning that the product (**14**) from addition of **13** to **9** would retain a primary amino group and therefore exhibit water solubility, enabling it to be removed from the reaction mixture by a simple aqueous extraction.[53] In the event, diamine **13** proved capable of completely removing **9** from the crude monomer mixture, affording a crude product that was enriched in the desired polymerizable

monomer **4** (Figure 4). After initially optimizing the reaction on small scale in dichloromethane, larger scale reactions (40 g of monomer mixture) were conducted neat.

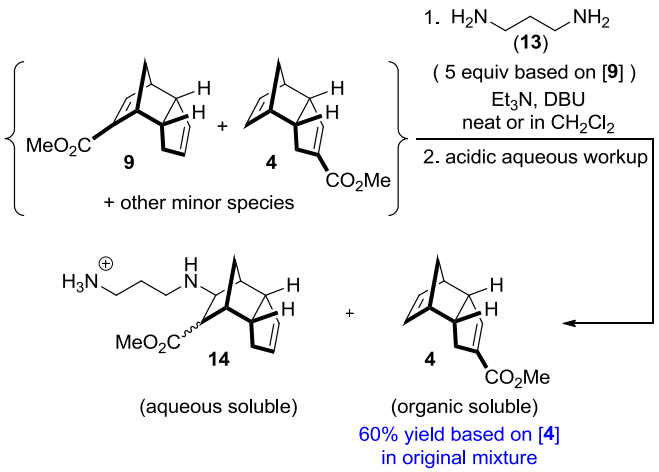

Figure 4. Selective removal of regioisomer **9** from the crude monomer mixture.

While the conjugate addition described above is sufficient to remove all of the undesired **9** from the reaction mixture (at least so far as can be detected by ^{1}H NMR), the mixture at this stage still contained other impurities, including minor isomer **10** (see below for further discussion and spectral details). In cases where the final monomer, **4**, was purified away from these impurities by column-chromatography, we found that a 60% overall yield (based upon the concentration of **4** in the original mixture, prior to conjugate addition) of highly purified monomer could be obtained following conjugate addition and chromatography.

With access thus established to large quantities of monomer **4** (with or without the presence of other regioisomers), we next investigated the development of a reaction-injection molding process that could be carried out either inside or outside the glove box, and would be compatible with the production of solid objects of suitable dimensions for dynamic mechanical analysis and other measurements.

Commercially available injection molding equipment is generally intended for larger-scale applications than we were interested in here, and is most commonly designed for use with thermoplastic polymers rather than thermosets. Even "bench-scale" injection molders therefore have significant dead-volumes associated with single- or twin-screw resin injection (which would lead to considerable wasted sample for us) and lack the ability to heat the mold after delivery of the sample (which is necessary for us to achieve crosslinking). In some senses, reaction injection molding of thermosets is simpler than traditional injection molding of thermoplastics, since monomers can be added to the mold in liquid state and therefore do not require heavy-duty pumps capable of dealing with highly viscous materials. The only caveat is that the mold should be resistant to the temperatures necessary to effect thermal curing.

Recognizing, then, that very simple molding apparatus could be used for our thermoset material, we constructed a mold from a stack of three rectangular pieces of aluminum. Desired shapes were cut into the center piece, while sprue holes were drilled in the top plate to permit addition of liquid monomer and catalyst, the combination of which could be easily added by syringe. The apparatus was easily assembled either in a fume hood or inside of a glove box, and could be firmly held together with clamps. Significantly, no special equipment was required either to construct the injection molding assembly or to use it in the laboratory. Pre-cut aluminum plates were ordered as needed from an online vendor, using CAD software to design our desired mold shapes. To highlight the utility of this process for shapes that are more complex than simple rectangular DMA samples, Figure 5 shows a mold used to prepare a version of our University's logo created entirely from *f*PDCPD.

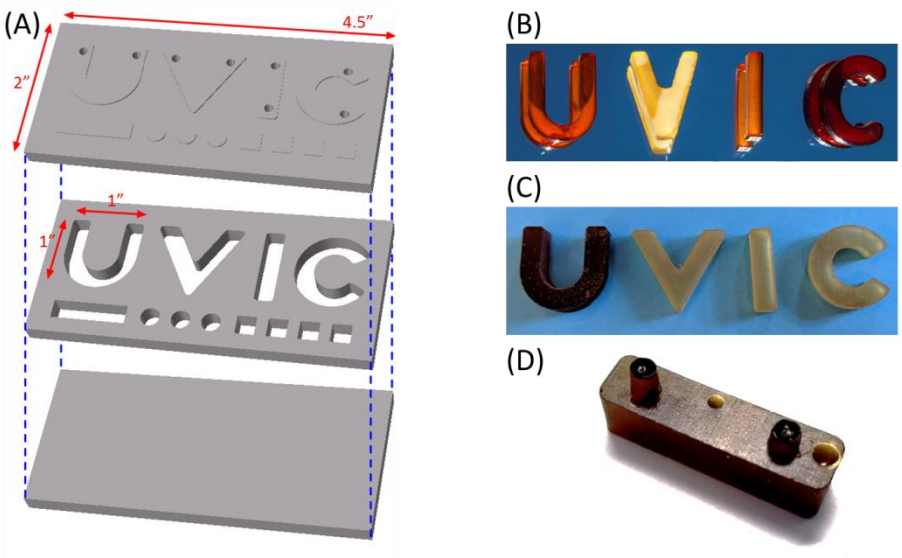

Figure 5. Reaction injection molding apparatus and representative molded *f*PDCPD products. (A) A laboratory-scale reaction injection molding apparatus comprised of three aluminum plates. The base plate is solid aluminum. Letters and other shapes have been cut through the center (molding) plate using a CNC mill. Sprue holes are drilled in the top plate to allow delivery of the polymer + catalyst mixture into the mold. The assembly is clamped during filling, polymerization, and thermal curing (clamps not shown). (B) Crosslinked *f*PDCPD objects prepared in silicone molds, photographed on a mirrored surface to illustrate the glassy appearance of the final products. The objects' irregular edges are due to the softness of the silicone molds. This is particularly visible for the letter 'I' which has noticeably curved sides. (C) Crosslinked *f*PDCPD objects produced using the aluminum mold described above. Much more consistent dimensions were achieved, although the surfaces have a somewhat roughened finish due to the use of unpolished aluminum for the molds. (D) A closeup of a letter 'I' made from crosslinked *f*PDCPD in an aluminum mold. Two small hemispherical voids are visible on the surface, presumably resulting from bubbles trapped within the mold. The cylindrical sprue features are *ca.* 3 mm in diameter. For all objects, darker colors indicate the use of longer crosslinking times.

Objects prepared using the aluminum mold were much more consistent than those obtained using earlier silicone and PLA molds. While small voids were still observed on the surface of the

final products (presumably resulting from bubbles), the overall quality of the samples was sufficient for DMA analysis, in that length, width, and height dimensions were consistent both across individual samples and between sample replicates.

The clamped mold could be easily filled by injection through the sprue holes of a pre-mixed suspension of **4** and an appropriate metathesis catalyst. The polymerization and crosslinking rates for **4** are sufficiently slow that we did not observe any clogging of the syringe needles that we used for injection. Conveniently, the thermal curing step can be accomplished without the need to remove the samples from the mold; the entire apparatus (including *f*PDCPD polymer, aluminum mold, and clamps) was simply transferred to an oven to effect crosslinking. At longer curing times, the samples became darker in color, but otherwise suffered no ill effects.

Dynamic Mechanical Analysis. With the ability to produce objects of regular dimensions, we next turned our attention to the rheological characterization of *f*PDCPD by dynamic mechanical analysis. In addition to comparing our ester-functionalized polydicyclopentadiene to unmodified dicyclopentadiene, we were curious to know how non-polymerizable impurities within the *f*DCPD monomer, **4**, might affect the performance of objects produced during a reaction injection molding process, where there is no opportunity for unreacted species to be removed from the final product.

As discussed above and illustrated in Figure 6, at different stages during the production of our target monomer we achieved mixtures of **4**, **9**, and **10** in various degrees of purity. Following the initial Diels–Alder dimerization of carboxylated cyclopentadiene (i.e. the protonated form of **8**) with unmodified cyclopentadiene, a mixture of products was observed including Thiele's ester **12** and dicyclopentadiene **11**. However, these two impurities were easy to remove, since the

former is relatively insoluble in hexanes while the latter can be distilled out of the product mixture. Following these two operations, the ^{1}H NMR spectrum indicates the presence of **9**, **10** and **4**, but relatively few other significant impurities (Figure 6C). Removal of isomer **9** by conjugate addition with diaminopropane affords a crude product that still contains **10** and **4** (Figure 6B), and final purification by flash-column chromatography provides pure desired product **4** (Figure 6A).

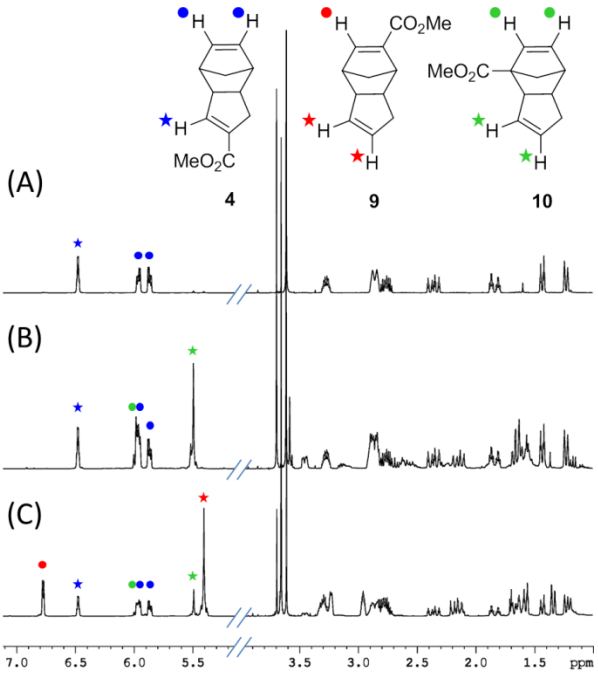

Figure 6. Representative ^{1}H NMR data for monomer **4** at various stages of the production process. (A) Column-purified compound **4**. (B) Product mixture after removal of regioisomer **9** by conjugate addition with diaminopropane, but prior to chromatography. Significant amounts of impurity **10** are present, along with other minor impurities. (C) Product mixture after initial formation by Diels–Alder dimerization and subsequent removal of dicyclopentadiene by distillation, but prior to conjugate addition with diaminopropane. Significant amounts of isomers **9** and **10** are both present.

We subjected each of these mixtures to our reaction injection molding protocol, to prepare samples for DMA. Each batch of monomer was polymerized in aluminum molds as described above. The polymerization was carried out in a glove box, using a 1% loading of the Grubbs second-generation catalyst. Comparator samples of unmodified polydicyclopentadiene were prepared identically. After polymerization, the molds were transferred directly to a 135 °C oven (under air) for either 24 hours or 6 days to effect thermal curing. We previously showed that increased thermal curing across this time regime dramatically increased crosslink density (i.e. decreased the average linear segment length between crosslinks).[29] After thermal curing, samples were removed and analyzed by DMA.

The storage and loss moduli for *f*PDCPD (prepared from column-purified **4**) and unmodified PDCPD were broadly similar (compare Figures 7A and 7C, or Figures 7B and 7D; overlays of storage moduli data shown in Figures 7E and 7F). The prepared *f*PDCPD samples showed a somewhat higher storage modulus at room temperature, but this decreased slightly with elevated temperature, while the unfunctionalized PDCPD samples actually increased slightly in modulus as the temperature was raised. These very minor differences in thermal behavior – which might be attributable to the packing of the ester groups within the polymer lattice – are probably less important than the fact that the data for *f*PDCPD and PDCPD align so closely with one another. Both are very high-modulus materials compared with other organic polymers, and exhibit relatively stable moduli across a broad temperature range. At least based upon the DMA data, then, the addition of the ester group does not appear to imperil the physical properties of polydicyclopentadiene. We also conducted Vickers hardness measurements on representative *f*PDCPD and PDCPD samples (Figure 8B). Consistent with the room-temperature modulus data, the *f*PDCPD samples exhibited a slightly higher hardness.

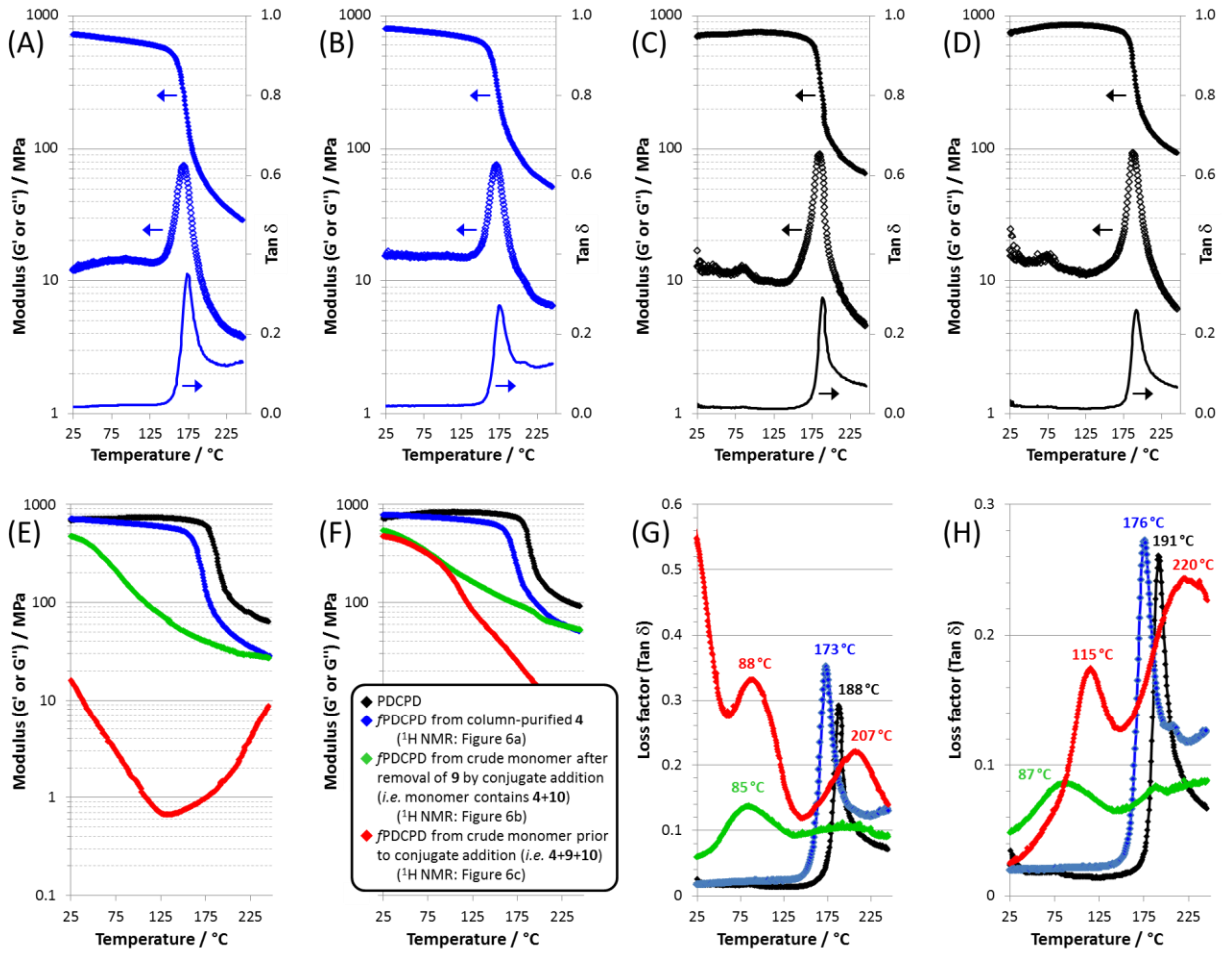

Figure 7. Results from DMA analysis of *f*PDCPD samples prepared with monomer samples of varying degrees of purity, compared with DMA results for unfunctionalized PDCPD. (A) *f*PDCPD from column-purified **4**, crosslinked for 24 hours at 135 °C. (B) *f*PDCPD from column-purified **4**, crosslinked for 6 days at 135 °C. (C) Unfunctionalized PDCPD, crosslinked for 24 hours at 135 °C. (D) Unfunctionalized PDCPD, crosslinked for 6 days at 135 °C. For panels A–D, data in blue corresponds to *f*PDCPD; data in black corresponds to unfunctionalized PDCPD; filled data points indicate storage modulus measurements (G′); open data points indicate loss modulus (G″); thin lines indicate loss factor (tan δ). (E) Comparison of storage modulus for PDCPD (black data), *f*PDCPD from column-purified **4** (blue data), *f*PDCPD from crude monomer after removal of **9** by conjugate addition (green data), and *f*PDCPD from crude monomer prior to conjugate addition (red data), where each sample was crosslinked for 24 hours at 135 °C. (F) Comparison of storage modulus for the four types of samples described in panel E, where each sample was crosslinked for 6 days at 135 °C. (G) Comparison of loss factor data for

the four types of samples described in panel E, where each sample was crosslinked for 24 hours at 135 °C. (H) Comparison of loss factor data for the four types of samples described in panel e, where each sample was crosslinked for 6 days at 135 °C. For panels G and H, numerical values indicate local maxima for each loss factor curve.

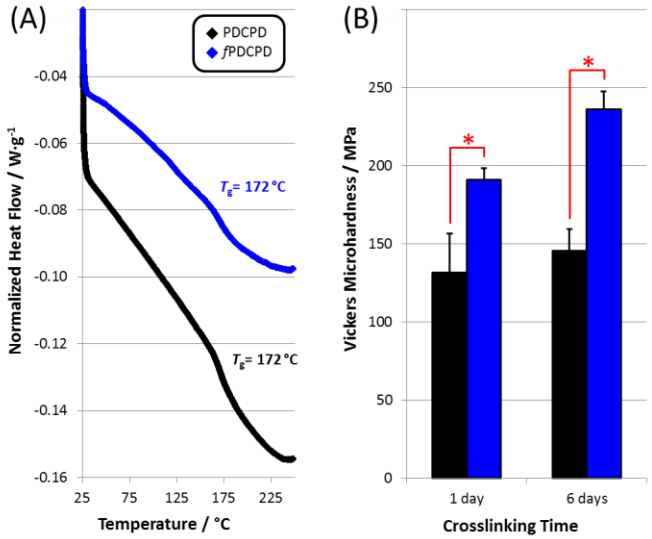

Figure 8. Comparison of DSC and Vickers hardness data for PDCPD (black) vs. *f*PDCPD (blue). (A) DSC data showing similar glass transition temperatures for the two samples. (B) Vickers hardness measurements showing an increase in hardness for *f*PDCPD relative to unfunctionalized PDCPD, and an increase in hardness with longer crosslinking times. Asterisks indicate statistical significance ($p < 0.05$). For both sets of measurements, *f*PDCPD was generated from column-purified monomer.

In earlier measurements of the glass transition temperature by DSC (using material prepared under somewhat different polymerization and crosslinking conditions) we found that *f*PDCPD samples displayed a consistently higher T_g (172 ± 3 °C) than that of unmodified PDCPD (155 – 165 °C).[28] In the present study, however, the DMA data revealed the opposite ordering of the tan δ maxima: as shown in Figures 7G and 7H, the apparent T_g in crosslinked

pure *f*PDCPD samples was about 15 °C lower than that for the crosslinked pure PDCPD samples. Glass transition temperature is not a constant for any material of course, and the apparent T_g will change with heating rate or analytical method. To better compare our current samples with those produced in our earlier work, we collected DSC data for samples prepared as described above. As shown in Figure 8A, our *f*PDCPD sample (made from column-purified ester **4**) and our in-house prepared PDCPD showed equivalent glass transition temperatures. While this is slightly different than what we had observed previously, the data once again serve to emphasize the similarities in the bulk properties of *f*PDCPD and PDCPD.

Not surprisingly, the modulus of our crosslinked polymer materials decreased with increasing concentrations of impurities in the monomer mixture. As shown in Figure 7E, low-purity *f*PDCPD prepared from the crude mixture of **4**, **9** and **10** (prior to conjugate addition with diaminopropane; ^{1}H NMR shown in Figure 6C) and crosslinked for 24 hours exhibited a storage modulus of only 16 MPa at room temperature (compared with 706 MPa for *f*PDCPD prepared from column-purified **4**, and 674 MPa for PDCPD prepared from commercial dicyclopentadiene). Removal of isomer **9** from the crude monomer mixture prior to polymerization and crosslinking (see Figure 6B for ^{1}H NMR of the input monomer, and green curve in Figure 7E for DMA data) greatly increased the modulus of the final product (to 471 MPa at room temperature), despite the fact that compound **10** is still present to act as a plasticizer.

Extended crosslinking times increased the storage modulus of all samples (compare Figure 7E to 7F), but the magnitude of the increase depended upon the provenance of the polymer material. The storage modulus of unmodified PDCPD increased from 674 to 732 MPa, while the same property for pure *f*PDCPD (i.e. prepared from column-purified **4**) increased similarly, from

706 to 782 MPa). The storage modulus of *f*PDCPD containing impurity **10** likewise experienced only a modest increase (from 471 MPa to 539 MPa), but the modulus of *f*PDCPD containing both **10** and **9** increased dramatically upon further crosslinking, from only 16 MPa after 24 hours, up to 470 MPa following a 6 day treatment. Indeed, at temperatures between 60 and 80 °C the moduli for the two impure forms of *f*PDCPD were virtually indistinguishable after 6 days of crosslinking.

Similar differential increases were observed in the maxima of the loss factor curves (Figures 7G and 7H). While the PDCPD and pure *f*PDCPD samples experienced only modest increases to the T_g in response to more extensive crosslinking, and while *f*PDCPD doped with **10** likewise showed very little change upon extended crosslinking, the sample of polymer containing both **9** and **10** (data shown in red) experienced a dramatic change to the loss factor curve with longer thermal curing time.

These data can be rationalized in light of the structures of the various species and what we know about the mechanism of polymerization and crosslinking. As we discussed above, **4** is the only monomer within the mixture capable of undergoing metathesis polymerization at room temperature. After the initial polymerization event, therefore, a polymer sample generated from a mixture of **4**, **9**, and **10** will now contain a mixture of linear polymer **5** together with unreacted **9** and **10** molecules that can function as plasticizers (see Figure 9). While the ratios of the three species vary somewhat from batch to batch, compound **9** is always the major product. Because of this, samples prepared from the crude monomer mixture – prior to removal of **9** by conjugate addition – will contain very large quantities of plasticizer and will therefore exhibit proportionately low storage moduli when thermal curing times are minimized. As discussed above, these samples are very pliable, and can be easily deformed by finger pressure.

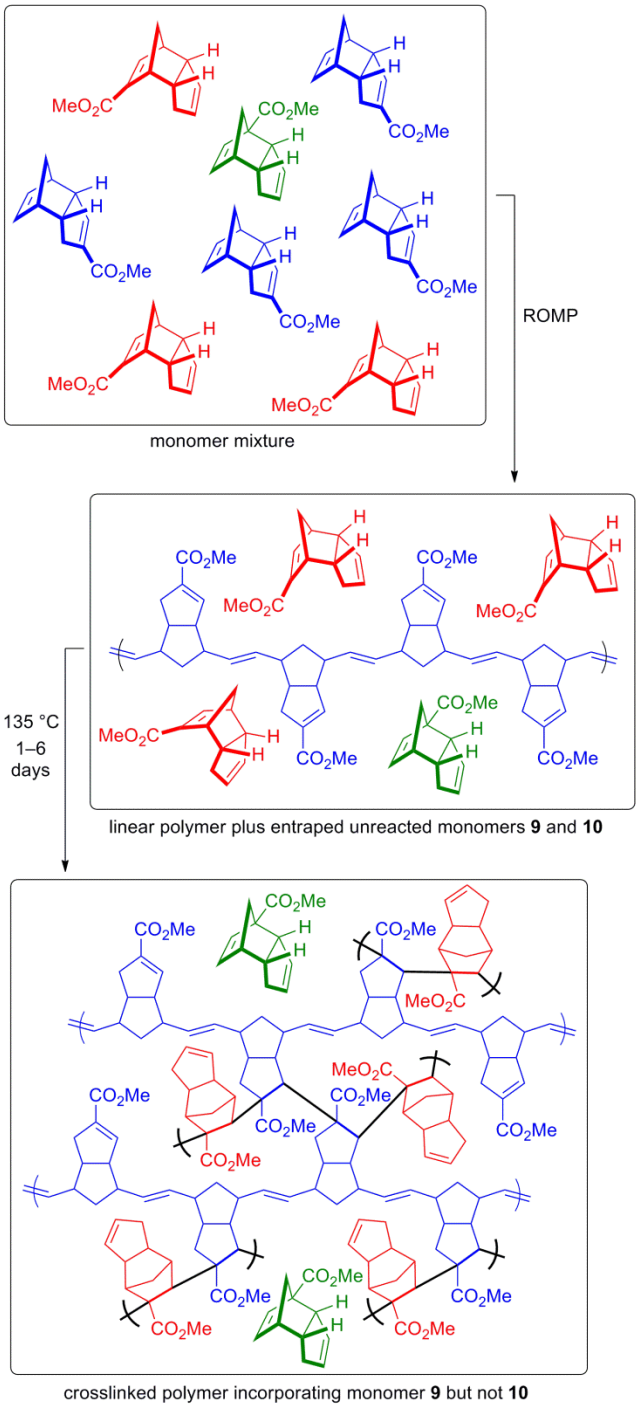

Figure 9. Proposal for the differential plasticizing effects of compounds **9** and **10** present in the crude monomer mixtures. Polymerizable monomer **4** (or polymer units derived from **4**) is shown in blue. Non-polymerizable, but crosslinkable, monomer **9** (or polymer units derived from **9**) is shown in red. Non-polymerizable and non-crosslinkable monomer **10** is shown in green. Key polymer crosslinks are indicated with bold black bonds.

We previously showed[29] that *f*PDCPD does not crosslink through secondary olefin metathesis events, but rather *via* head–tail olefin addition polymerization, wherein the methyl methacrylate motif embedded within one residue along the polymer chain adds to the methyl methacrylate motif on a second residue – either on the same chain or (more likely) on a neighboring chain. Critically, compound **9** contains a methacrylate group (an α,ß-conjugated ester) but compound **10** does not! This fundamental difference explains the differential behavior of polymer samples prepared with or regioisomer **9**.

When thermally cured, entrapped compound **9** can participate in the olefin addition crosslinking events, even though it did not participate in the original polymerization. As shown in Figure 9, then, a polymer that once contained a low crosslink density and large amounts of plasticizer becomes transformed into a highly crosslinked material. A large increase in storage modulus would be expected following this transformation, which is consistent with the observed result.

By contrast, **10** cannot participate in either the olefin metathesis polymerization reaction, *or* the olefin addition crosslinking process. It likely remains as a spectator (and therefore plasticizer) even after lengthy thermal curing protocols. This explains why the modulus of polymer doped with **10** (green data in Figure 7) never 'catches up' to that of polymer prepared without this impurity, even at long crosslinking times. It also explains why polymer prepared with both **10** and **9** present (red data in Figure 7) eventually exhibits very similar modulus values to polymer prepared with only **10** present: after a sufficiently long crosslinking time both samples contain about the same amount of residual plasticizer.

While these explanations necessarily include a certain degree of *post hoc* rationalization of the experimental data, they nonetheless provide a useful conceptual framework for designing and preparing additional types of functionalized polydicyclopentadiene materials that encompass a broader range of properties (storage modulus, surface energy, T_g, etc.) than has been available in the past.

CONCLUSIONS

In this work we have made several important contributions toward the broader usage of functionalized forms of dicyclopentadiene (DCPD).

We first demonstrated several improvements to the synthesis of the monomer mixture that leads to *C*-linked ester-functionalized polydicyclopentadiene (*f*PDCPD), and showed that pure linear polymer could be produced from this crude mixture through selective ring-opening metathesis polymerization. The ability to access pure linear (and thus crosslinked) *f*PDCPD without the need for column chromatography represents a significant improvement over our previous work.

Secondly, we showed that our synthetic protocols were capable of producing the functionalized dicyclopentadiene monomer mixture on >450-gram scale, and we developed a new protocol to remove the principal unwanted species from within this mixture through conjugate addition. This reaction also works on large scale, without additional solvent, and provides product of respectable purity even before chromatography.

Thirdly – and perhaps most significantly – we took advantage of the increased amounts of our materials to develop a reaction injection molding protocol that could be used inside a standard laboratory glove box without the need for specialized equipment.[54] This led to the first production of macro-scale objects from our *C*-linked ester-functionalized PDCPD polymer, which we then used in a series of dynamic mechanical analysis experiments aimed at comparing the mechanical properties of *f*PDCPD to those of traditional unfunctionalized PDCPD. The Lemcoff group has also conducted DMA analysis of their allylically-functionalized PDCPD materials;[21] as noted above these tended to have lower T_g values as well as lower decomposition temperatures.

While we had previously shown that our vinyl-functionalized *f*PDCPD exhibited nearly identical thermal stability to traditional PDCPD together with an increased T_g (when measured by differential scanning calorimetry), here we showed for the first time that the two polymers are also equivalent in terms of their storage and loss moduli. Given that polydicyclopentadiene is most valued for its excellent material strength, these modulus measurements are arguably the most important piece of data yet in supporting the use of *f*PDCPD in applications that are currently reserved for traditional PDCPD. Indeed, since we have already shown a greatly increased and tunable surface energy associated with *f*PDCPD relative to PDCPD (with γ_{sv} values ranging from 38.5 mN/m up to 66.6 mN/m),[28] we anticipate that this new material can be used in a broader range of applications than is currently open to the unfunctionalized polymer.

Significantly, while chromatographically purified monomer was used to obtain crosslinked polymer with the highest measured storage modulus, we also found that unpurified monomer could still provide a respectably high-modulus material (G' > 500 MPa at 25 °C) without the need for any chromatography steps throughout the entire production process. Thus, while further

advances toward the selective synthesis of monomer **4** will no doubt be required to support the large scale production of the target polymer, the results described herein strongly support the utility of new, functionalized forms of polydicyclopentadiene.

EXPERIMENTAL SECTION

Large-scale synthesis of regioisomeric monomer mixture. Freshly cracked cyclopentadiene (272.04 g, 4.12 mol), was slowly added to a solution of NaH (99 g, 4.12 mol) in dried tetrahydrofuran (THF, 2.06 L) at 0 °C over 1 hour. Dimethylcarbonate (1750 mL, 20.6 mol) was then added to the resulting 2M NaCP solution and the mixture was heated to 40 °C for 12 hours. Volatiles were removed *in vacuo*, and freshly cracked cyclopentadiene (544.08 g, 8.24 mmol), isopropanol (3 L) and H_2SO_4 (140 mL, 2.58 mol, 0.6 equiv.) were added. The mixture was stirred for 48 hours. Volatiles were then removed *in vacuo* and the resulting black mixture was dissolved in hexanes and washed with deionized water. Volatiles were then removed *in vacuo*, affording an oil. This oil was then heated at 50 °C under vacuum (0.1 mmHg) for 4 hours to remove all remaining dicyclopentadiene, resulting in a black oil. Yield: 468 g, 60%; as a crude mixture of regioisomers **4**, **9** and **10**. Spectroscopic data for **4** and **9** was identical to that reported previously.[28,29] Spectroscopic data for **10** is provided in the Supporting Information.

Removal of isomer 9 through conjugate addition with 1,3-diaminopropane. 40 g of the unpurified mixture of monomers described above (after removal of residual dicyclopentadiene at 50 °C and 0.1 mm Hg) was stirred in a round-bottom flask. The non-polymerizable regioisomer (~23 g, 0.12 mol) was reacted by adding triethylamine (92.4 mL, 5 equiv.), DBU (9.8 mL, 0.5 equiv.), and 1,3-diaminopropane (58.1 mL, 5 equiv.) at 0 °C with stirring for 24 hours under

argon. The resulting mixture was dissolved in diethyl ether and washed with 1M HCl, followed by saturated aqueous $NaHCO_3$ and saturated aqueous NaCl. Volatiles were removed *in vacuo*, resulting in the isolation of a dark brown oil. The oil was dried under high vacuum to remove solvent residue, affording 16 g (> 90% recovery) of a crude mixture of regioisomers **4** and **10**.

Chromatographic purification of monomer 4. The crude mixture of **4** and **10** (following removal of **9** with 1,3-diaminopropane) was dissolved in hexanes and loaded onto a silica gel column. Elution with 20:1 hexanes:ethyl acetate followed by concentration *in vacuo* provided monomer **4** as a light yellow oil with an estimated purity (by NMR) of $\geq$ 90%. Spectroscopic data was identical to that reported previously.[28,29]

Reaction injection molding of monomer 4. Functionalized dicyclopentadiene **4** (purified as indicated above) was combined under inert atmosphere in a glove box with the Grubbs second generation catalyst (1 mol %) in a glass vial. The mixture was stirred with a spatula for 30 seconds, then taken up in a plastic syringe, and immediately transferred through sprue holes (~3 mm) cut into a ¼" aluminum top plate, into an aluminum mold with a depth of ¼". Test samples prepared in this way had a height of approximately 1" and a variable width and shape, as indicated in Figure 5. The samples were allowed to polymerize for 24 hours at room temperature in the glove box, after which the mold (still containing the polymer samples) was removed from the glove box and placed in an oven at 135 °C to effect thermal curing. Different curing times (30 minutes to 24 hours) provided samples with different degrees of coloring. The mold was then disassembled by removing the top and bottom plates, and the samples were removed. To facilitate removal of the polymer samples, the aluminum mold (as well as the associated top and bottom plates) was treated with a Teflon-containing spray prior to use.

Mechanical measurements. Samples of pure functionalized or nonfunctionalized polydicyclopentadiene were prepared as described above, and tested by dynamic mechanical thermal analysis (DMTA) on an Anton Paar MCR 302 rheometer with SRF 12 geometry and CTD 600 oven. Frequency and amplitude sweeps were completed to ensure testing parameters for temperature-sweep measurements were within the viscoelastic region (Figure S19). Temperature-sweep measurements were performed with a strain of 0.1%, a frequency of 1 Hz, and a heating rate of 1 °C/min. Tested samples were solid rectangular bars of dimensions 12 mm x 4 mm x 25 mm. Complementary hardness tests were completed on a Buehler Wilson VH 3100 instrument with a Vickers diamond shaped indenter. Tested samples were solid cylinders with a height of 14.5 mm and diameter of 14.5 mm. DSC analysis was conducted using a heating rate of 10 °C/min.

ASSOCIATED CONTENT

Supporting Information.

The Supporting Information is available free of charge on the ACS Publications website at DOI: Supplementary figures; spectral data for compound **10**; control experiments for DMTA measurements (PDF).

AUTHOR INFORMATION

Corresponding Author

*E-mail: wulff@uvic.ca.

Author Contributions

† T.J.C. and T.L. contributed equally to this work, and are listed in alphabetical order.

Funding Sources

Operating funds for this work came from an NSERC Idea to Innovation grant (#501981-16) to J.W. The rheometer used for DMA analysis was purchased with funds from an NSERC Research Tools and Instruments grant, for which J.W. was a co-applicant. Partial salary support for J.W. was provided by the Canada Research Chairs program.

Conflict of Interest Declaration

J.W., T.J.C., and T.L. are co-inventors on US patent application no. 15/999,209, which claims the use of the polymer described herein.

ACKNOWLEDGMENTS

The authors thank Dr. Mathieu Lepage for collecting the DSC data shown in Figure 8A, and Mr. Ryan Mandau for collecting the hardness data shown in Figure 8B. The research team also wishes to extend its gratitude to Ms. Ella Guan for the photo used for the graphical abstract to this work, as well as photos of injection molded objects used in Figures 5B and 5C.

REFERENCES

(1) Fischer, I.; Schmitt, W. F.; Porth, H.-C.; Allsopp, M. W.; Vianello, G. Poly(Vinyl Chloride) in *Ullmann's Encyclopedia of Industrial Chemistry*, Wiley-VCH, Weinheim, Germany **2014**.

(2) AGPU press release, 2016. Everything About PVC from Manufacturing to Recycling, www.agpu.de, accessed December, **2018**.

(3) Wagoner, J. K. Toxicity of Vinyl Chloride and Poly(vinyl chloride): a Critical Review. *Environ. Health Perspect.* **1983**, *52*, 61–66.

(4) Todd, G. D.; Faroon, O. M.; Jones, D. E.; Lumpkin, M. H.; Stickney, J.; Citra, M. J. Toxicological Profile for Vinyl Chloride, U.S. Department of Health and Human Services, Atlanta, Georgia, USA **2006**.

(5) McCombie, G.; Biedermann, S.; Suter, G.; Biedermann, M. Survey on Plasticizers Currently Found in PVC Toys on the Swiss Market: Banned Phthalates are Only a Minor Concern. *J. Environ. Sci. Health A* **2017**, *52*, 491–496.

(6) Zhai, Y.; Zhao, J.; Di, X.; Di, S.; Wang, B.; Yue, Y.; Sheng, G.; Lai, H.; Guo, L.; Wang, H.; Li, X. Carbon-supported Perovskite-like $CsCuCl_3$ Nanoparticles: a Highly Active and Cost-effective Heterogeneous Catalyst for the Hydrochlorination of Acetylene to Vinyl Chloride. *Catal. Sci. Technol.* **2018**, *8*, 2901–2908.

(7) Scharfe, M.; Lira-Parada, P. A.; Paunović, V.; Moser, M.; Amrute, A. P. Pérez-Ramírez, J. Oxychlorination–Dehydrochlorination Chemistry on Bifunctional Ceria Catalysts for Intensified Vinyl Chloride Production. *Angew. Chem. Int. Ed.* **2016**, *55*, 3068–3072.

(8) Lamberti, C.; Prestipino, C.; Bonino, F.; Capello, L.; Bordiga, S.; Spoto, G.; Zecchina, A.; Moreno, S. D.; Cremaschi, B.; Garilli, M.; Marsella, A.; Carmello, D. Vidotto, S.; Leofanti, G. The Chemistry of the Oxychlorination Catalyst: an In Situ, Time-Resolved XANES Study. *Angew. Chem. Int. Ed.* **2002**, *41*, 2341–2344.

(9) Long, T. R.; Elder, R. M.; Bain, E. D.; Masser, K. A.; Sirk, T. W.; Yu, J. H.; Knorr Jr., D. B.; Lenhart, J. L. Influence of Molecular Weight Between Crosslinks on the Mechanical Properties of Polymers Formed via Ring-opening Metathesis. *Soft Matter* **2018**, *14*, 3344–3360.

(10) Knorr, Jr., D. B.; Masser, K. A.; Elder, R. M.; Sirk, T. W.; Hindenlang, M. D.; Yu, J. H.; Richardson, A. D.; Boyd, S. E.; Spurgeon, W. A.; Lenhart, J. L. Overcoming the Structural Versus Energy Dissipation Trade-off in Highly Crosslinked Polymer Networks: Ultrahigh Strain Rate Response in Polydicyclopentadiene. *Compos. Sci. Technol.* **2015**, *114*, 17–25.

(11) Vervacke, D. *An Introduction to PDCPD*, Product Rescue, Waarschoot, Belgium, **2008**.

(12) Della Martina, A.; Garamszegi, L.; Hilborn, J. G. Pore Size Modification of Macroporous Crosslinked Poly(dicyclopentadiene). *J. Polym. Sci., Part A: Polym. Chem.* **2003**, *41*, 2036–2046.

(13) Mol, J. C. Industrial Applications of Olefin Metathesis *J. Mol. Catal. A: Chem.* **2004**, *213*, 39–45.

(14) Matějka, L.; Houtman, C.; Macosko, C. W. Polymerization of Dicyclopentadiene: A New Reaction Injection Molding System. *J. Polym. Sci.* **1985**, *30*, 2787–2803.

(15) Ng, H.; Manas-Zloczower, I.; Shmorhun, M. Rheokinetic Studies for the Reaction Injection Molding of Polydicyclopentadiene. *Polym. Eng. Sci.* **1994**, *34*, 921–928.

(16) Ng, H.; Manas-Zloczower, I. Moldability Studies for the Reaction Injection Molding of Polydicyclopentadiene. *Polym. Eng. Sci.* **1994**, *34*, 929–936.

(17) Wang, L.; Pan, B.; Du, J.; Cheng, Y.; Liu, J.; Du, S.; Shangguan, B.; Zhang, Y. The Tribological and Mechanical Properties of PDCPD/PEW Composites Prepared by Reaction Injection Moulding. *Polym. Polym. Compos.* **2015**, *23*, 37–41.

(18) Perwuelz, A.; Campagne, C.; Lam, T. M. Caractérisation de la Surface du Polydicyclopentadiene (Poly-DCPD): Influence du Vieillissement sur le Mouillage et l'Adhesion de Peinture. *J. Chim. Phys.* **1999**, *96*, 904−922.

(19) Stehmeier, L. G.; Francis, M. M.; Jack, T. R.; Voordouw, G. Biodegradation of Dicyclopentadiene in the Field. *Biodegradation* **1999**, *10*, 135–148.

(20) Hine, P. J.; Leejarkpai, T.; Khosravi, E.; Duckett, R. A.; Feast, W. J. Structure Property Relationships in Linear and Cross-linked Poly(imidonorbornenes) Prepared Using Ring Opening Metathesis Polymerisation (ROMP). *Polymer* **2001**, *42*, 3413–9422.

(21) Saha, S.; Ginzburg, Y.; Rozenberg, I.; Iliashevsky, O.; Ben-Asuly, A.; Lemcoff, N. G. Cross-linked ROMP Polymers Based on Odourless Dicyclopentadiene Derivatives. *Polym. Chem.* **2016**, *7*, 3071–3075.

(22) García, J. M.; Jones, G. O.; Virwani, K.; McCloskey, B. D.; Boday, D. J.; ter Huurne, G. M.; Horn, H. W.; Coady, D. J.; Bintaleb, A. M.; Alabdulrahman, A. M. S.; Alsewailem, F.; Almegren, H. A. A.; Hedrick, J. L. Recyclable, Strong Thermosets and Organogels via Paraformaldehyde Condensation with Diamines. *Science* **2014**, *344*, 732–735.

(23) Perring, M.; Bowden, N. B. Assembly of Organic Monolayers on Polydicyclopentadiene. *Langmuir* **2008**, *24*, 10480–10487.

(24) Perring, M.; Long, T. R.; Bowden, N. B. Epoxidation of the Surface of Polydicyclopentadiene for the Self-assembly of Organic Monolayers. *J. Mater. Chem.* **2010**, *20*, 8679–8685.

(25) Knall, A.-C.; Kovačič, S.; Hollauf, M.; Reishofer, D.; Saf, R.; Slugovc, C. Inverse Electron Demand Diels–Alder (iEDDA) Functionalisation of Macroporous Poly(dicyclopentadiene) Foams. *Chem. Commun.* **2013**, *49*, 7325–7327.

(26) Kovačič, S.; Krajnc, P.; Slugovc, C. Inherently Reactive PolyHIPE Material from Dicyclopentadiene. *Chem. Commun.* **2010**, *46*, 7504–7506.

(27) Gong, L.; Liu, K.; Ou, E.; Xu, F.; Lu, Y.; Wang, Z.; Gao, T.; Yang, Z.; Xu, W. ROMP of Acetoxy-substituted Dicyclopentadiene to a Linear Polymer with a High T_g. *RSC Adv.* **2015**, *5*, 26185–26188.

(28) Chen, J.; Burns, F. P.; Moffitt, M. G.; Wulff, J. E. Thermally Crosslinked Functionalized Polydicyclopentadiene with a High T_g and Tunable Surface Energy. *ACS Omega* **2016**, *1*, 532–540.

(29) Cuthbert, T. J.; Li, T.; Speed, A. W. H.; Wulff, J. E. Structure of the Thermally Induced Cross-Link in *C*-Linked Methyl Ester-Functionalized Polydicyclopentadiene (*f*PDCPD). *Macromolecules* **2018**, *51*, 2038–2047.

(30) Steese, N. D.; Barvaliya, D.; Poole, X. D.; McLemore, D. E.; DiCesare, J. C.; Schanz, H.-J. Synthesis and Thermal Properties of Linear Polydicyclopentadiene via Ring-opening

Metathesis Polymerization with a Third Generation Grubbs-type Ruthenium-alkylidene Complex. *J. Polym. Sci., Part A: Polym. Chem.* **2018**, *56*, 359–364.

(31) Yao, Z.; Wang, Z.; Yu, Y.; Zeng, C.; Cao, K. Facile Synthesis and Properties of the Chemo-reversible and Highly Tunable Metallogels based on Polydicyclopentadiene. *Polymer* **2017**, *119*, 98–106.

(32) Abadie, M. J.; Dimonie, M.; Couve, C.; Dragutan, V. New Catalysts for Linear Polydicyclopentadiene Synthesis. *Eur. Polymer J.* **2000**, *36*, 1213–1219.

(33) Dragutan, V.; Dragutan, I.; Dimonie, M.; Abadie, M. J.; Couve, J. Selective Synthesis of Linear Polydicyclopentadiene with Tungsten-based ROMP Catalysts. *Polymer Preprints* **2001**, *42*, 457–458.

(34) Goetz, A. E.; Boydston, A. J. Metal-Free Preparation of Linear and Cross-Linked Polydicyclopentadiene. *J. Am. Chem. Soc.* **2015**, *137*, 7572–7575.

(35) Davidson, T. A.; Wagener, K. B. The Polymerization of Dicyclopentadiene: an Investigation of Mechanism. *J. Mol. Catal. A Chem.* **1998**, *133*, 67–74.

(36) Davidson, T. A.; Wagener, K. B.; Priddy, D. B. Polymerization of Dicyclopentadiene: A Tale of Two Mechanisms. *Macromolecules* **1996**, *29*, 786–788.

(37) Hsu, H.-C.; Wang, S.-J.; Ou, J. D.-Y.; Wong, D. S. H. Simplification and Intensification of a C5 Separation Process. *Ind. Eng. Chem. Res.* **2015**, *54*, 9798–9804.

(38) Nurullina, E. V.; Solov'eva, N. B.; Liakumovich, A. G.; Samuilov, Y. D. Production of High-Purity Dicyclopentadiene from the C5 Fraction of Hydrocarbon Pyrolysis. *Russ. J. Appl. Chem.* **2001**, *74*, 1590–1593.

(39) Chen, J.; Kilpatrick, B.; Oliver, A. G.; Wulff, J. E. Expansion of Thiele's Acid Chemistry in Pursuit of a Suite of Conformationally Constrained Scaffolds. *J. Org. Chem.* **2015**, *80*, 8979–8989.

(40) Chen, J.; Lu, L.; Wulff, J. E. Radical Stabilization Algorithm as a Predictive Tool for Novel and Reported Noncanonical Thiele's Acid Analogues. *Synlett* **2017**, *29*, 2777–2782.

(41) Chen, J.; Wulff, J. E. Revisiting the Mechanistic Origins of Thiele's ester Dimerization: Probing the Reliability of Predictive Models for Cycloadditions. *Org. Biomol. Chem.* **2016**, *14*, 10170–10174.

(42) A small amount of dark-colored oily byproduct excluded by the hexanes fraction *did* impair the function of the catalyst if it were left within the reaction mixture, but this could be removed by simply using hexanes as the organic solvent in the aqueous workup step.

(43) At the scale we were working at, we found it convenient to generate NaCp ourselves from sodium hydride and freshly cracked cyclopentadiene. At either smaller or larger scales, however, it would generally be more convenient to source NaCp commercially. With this in mind, we prepared our NaCp solution to be 2 M in THF, which is typical of commercial concentrations used by vendors of both small (e.g. Sigma) and large (e.g. Boulder Scientific) quantities.

(44) Ester-containing species **4** and **9** do not begin to distil until approximately 5 °C higher in temperature.

(45) With 0.1% catalyst loadings, the polymerization was noticeably slower than with 1% catalyst loadings. Although it was difficult to determine the exact rate of polymerization (as

discussed in the text), we typically let these low-catalyst reactions run for 24 hours to ensure completion.

(46) Takeuchi, Y.; Ono, Y.; Hisanaga, N.; Kitoh, J.; Sugiura, Y. A Comparative Study on the Neurotoxicity of n-Pentane, n-Hexane, and n-Heptane in the Rat. *Br. J. Ind. Med.* **1980**, *37*, 241–247.

(47) U.S. EPA, IRIS Toxicological Review and Summary Documents for n-Hexane (External Review Draft), U.S. Environmental Protection Agency, Washington, D.C., **2005**.

(48) Daughtrey, W.; Newton, P.; Rhoden, R.; Kirwin, C.; Haddock, L.; Duffy, J.; Keenan, T.; Richter, W.; Nicolich, M. Chronic Inhalation Carcinogenicity Study of Commercial Hexane Solvent in F-344 Rats and B6C3F1 Mice. *Toxicol. Sci.* **1999**, *48*, 21–29.

(49) Goel, S. K.; Rao, O. S.; Pandya, K. P. Toxicity of n-Hexane and n-Heptane: Some Biochemical Changes in Liver and Serum. *Toxicology Lett.* **1982**, *14*, 169–174.

(50) Yang, Y.-S.; Lafontaine, E.; Mortaigne, B. NMR Characterisation of Dicyclopentadiene Resins and Polydicyclopentadienes. *J. Appl. Polymer Sci.* **1996**, *60*, 2419–2435.

(51) McGann, C. L.; Daniels, G. C.; Giles, S. L.; Balow, R. B.; Miranda-Zayas, J. L.; Lundin, J. G.; Wynne, J. H. Air Activated Self-Decontaminating Polydicyclopentadiene PolyHIPE Foams for Rapid Decontamination of Chemical Warfare Agents. *Macromol. Rapid Commun.* **2018**, *39*, 1800194.

(52) Peters, D. Simple Derivatives of Cyclopentadiene. Part III. The Adducts of Methyl Cyclopentadienecarboxylate and Cyclopentadiene *J. Chem. Soc.* **1961**, 1037–1042.

(53) Although developed primarily for scale-up purposes, this reaction was also employed in our recent spectroscopic study of the crosslinking structure in polymer **6**. See reference 29 for details.

(54) The polymerization of *f*PDCPD can be accomplished outside a glove box too, but we were concerned that traces of oxygen in the sample might lead to inconsistent DMA results. As discussed above, all forms of PDCPD are prone to oxidation. Since one of our primary objectives in the current work was to compare the storage moduli of PDCPD and *f*PDCPD, we decided out of an abundance of caution to carry out all of our polymerizations in the glove box.

TOC/ABSTRACT GRAPHIC

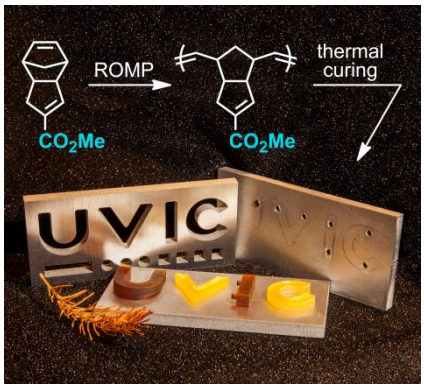

Supporting Information for:

Production and Dynamic Mechanical Analysis of Macro-Scale Functionalized Polydicyclopentadiene Objects Facilitated by Rational Synthesis and Reaction Injection Molding

*Tyler J. Cuthbert, Tong Li, and Jeremy E. Wulff**

Department of Chemistry, University of Victoria, PO Box 3065 STN CSC, Victoria, British Columbia, V8W 3V6, Canada

**Corresponding Author: wulff@uvic.ca*

Index

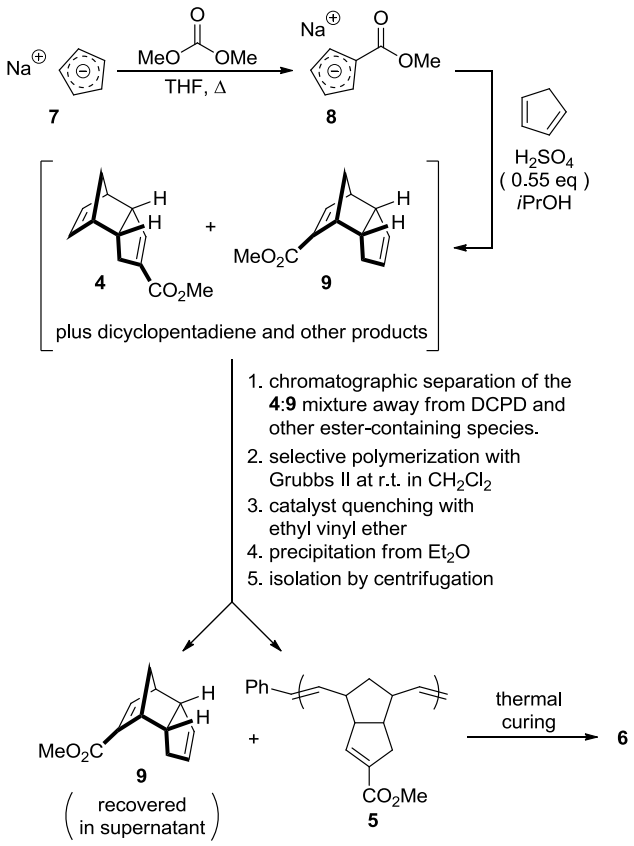

Figure S1. Previous method for producing *f*PDCPD, based on selective polymerization from a chromatographically purified monomer mixture.

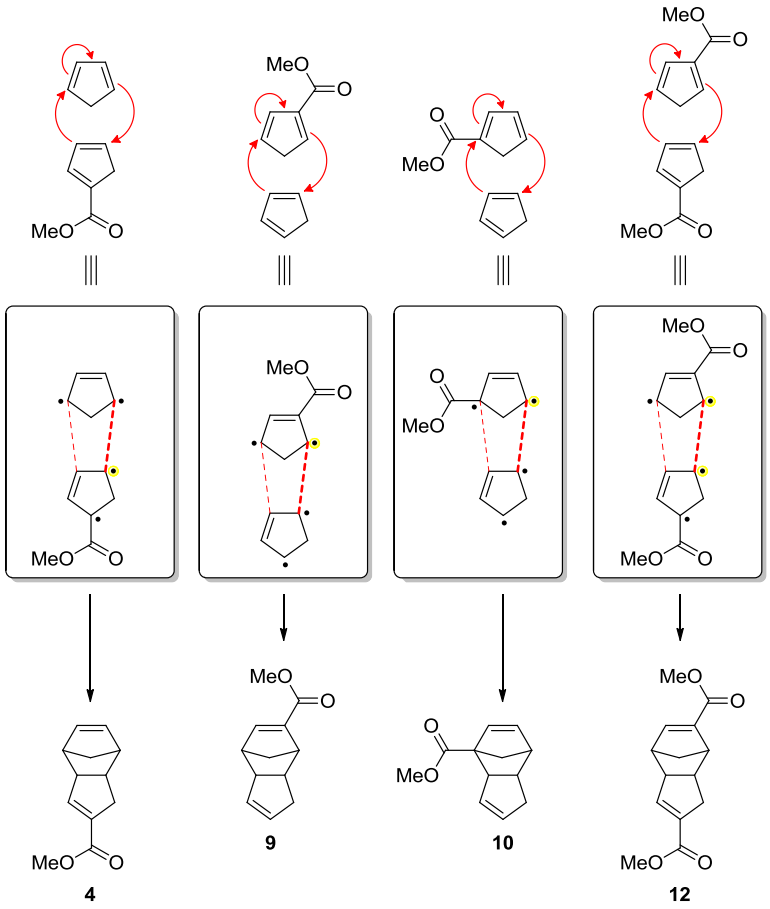

Figure S2. The regiochemical outcome for the Diels–Alder reactions leading to each of the ester-functionalized dicyclopentadienes **4**, **9**, **10**, and **12** (as well as the unfunctionalized dicyclopentadiene **11**, not shown), is consistent with our earlier prediction of regiochemistry using radical stabilization arguments.[40,41] Briefly, these arguments require that each diene species be viewed as its corresponding 1,4-diradical resonance structure. The fastest Diels–Alder coupling is then predicted to arise through the coupling of the least-stabilized radicals (highlighted in yellow in the Figure). The characterization of the new compound **10** (which was not known at the time of our earlier publications) therefore further supports these arguments.

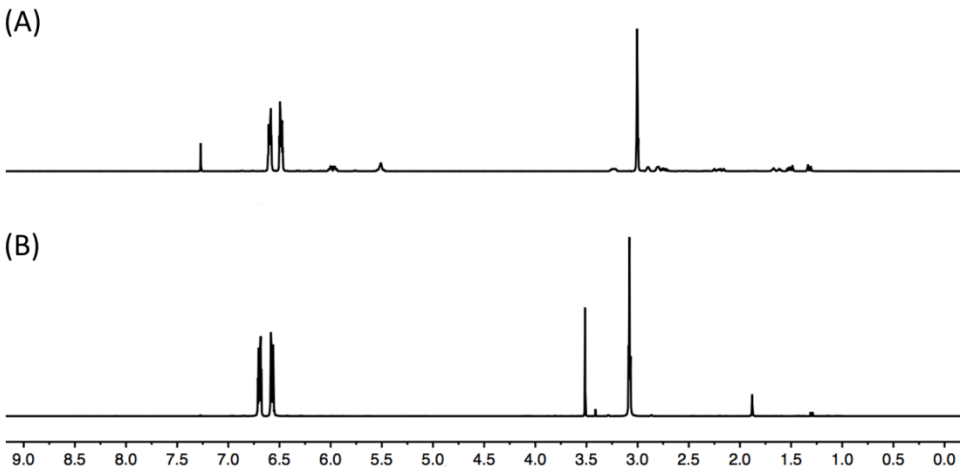

Figure S3. Comparison of ^{1}H NMR spectrum for dicyclopentadiene recovered by distillation (A) to a spectrum for commercial dicyclopentadiene (B).

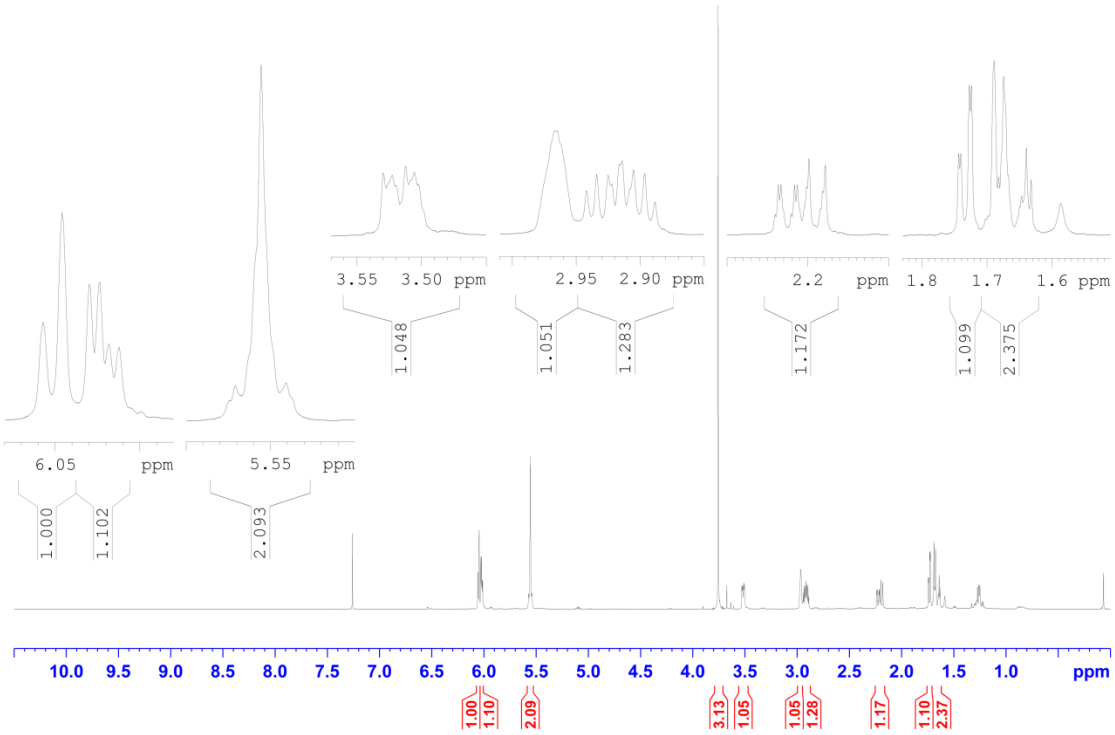

Figure S4. ^{1}H NMR spectrum for compound **10** in $CDCl_3$, recorded at 500 MHz.

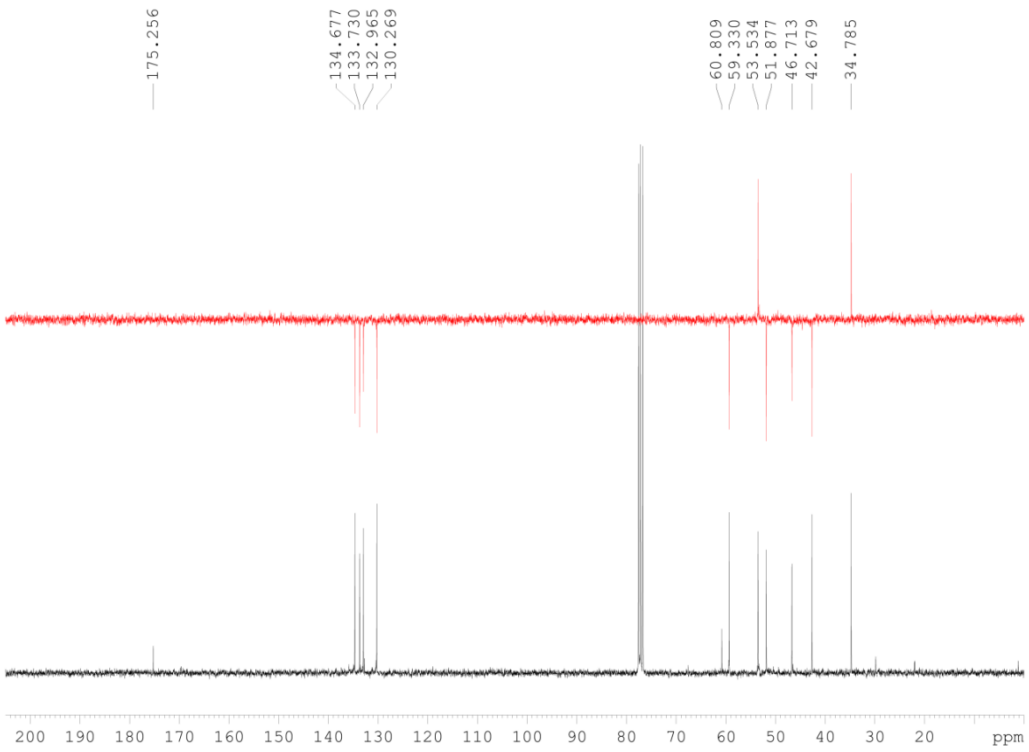

Figure S5. ^{13}C NMR and DEPT-135 NMR spectra (in black and red, respectively) for compound **10** in $CDCl_3$, recorded at 75 MHz.

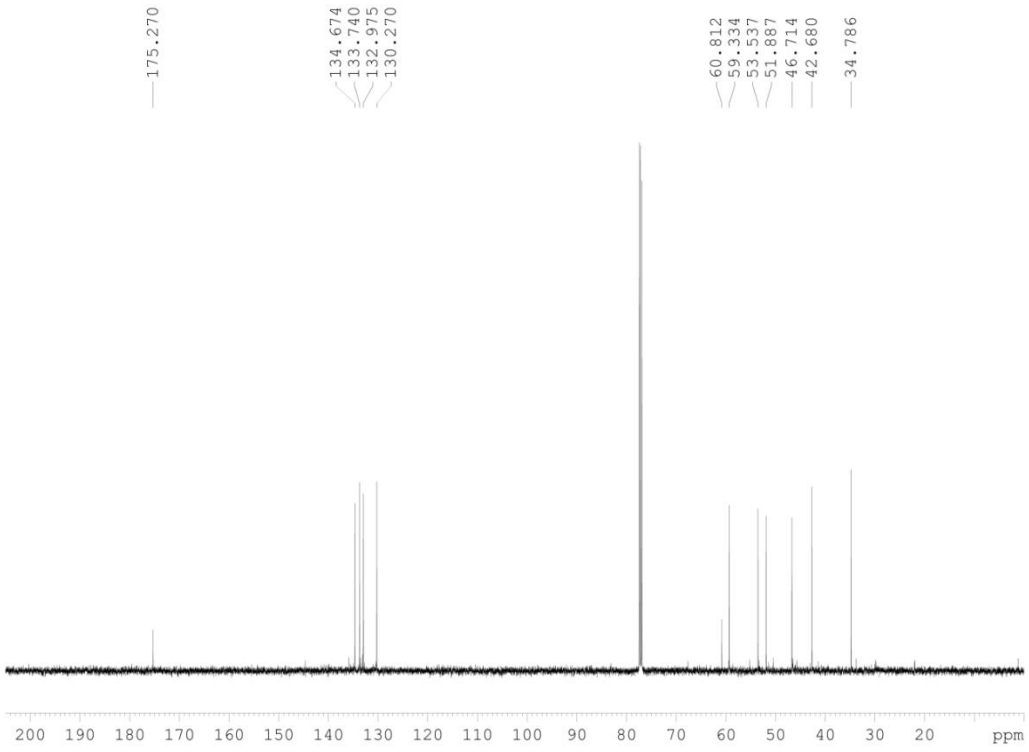

Figure S6. ^{13}C NMR NMR spectrum for compound **10** in $CDCl_3$, recorded at 125 MHz.

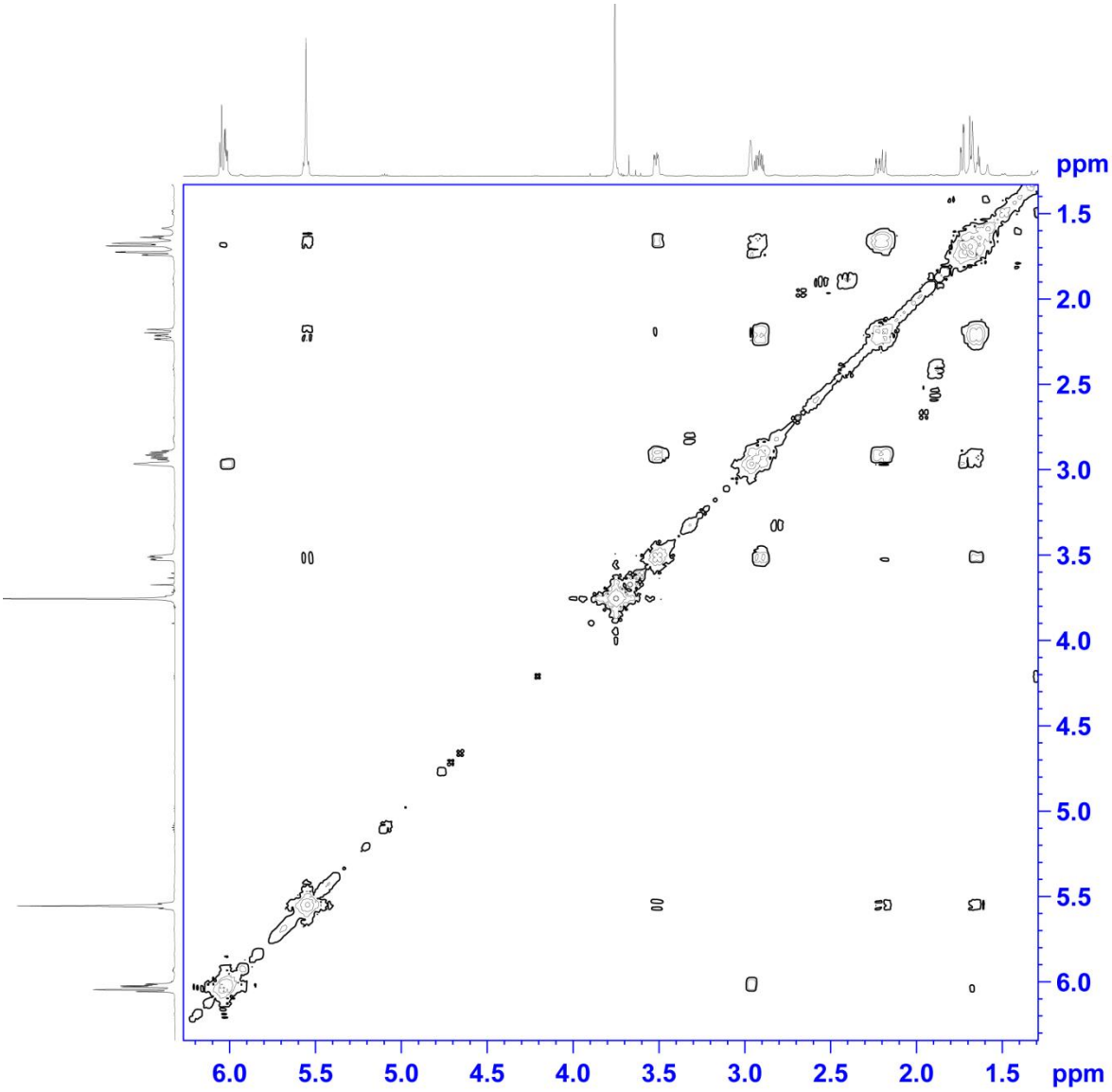

Figure S7. COSY NMR spectrum (full range) for compound **10** in $CDCl_3$, recorded at 500 MHz.

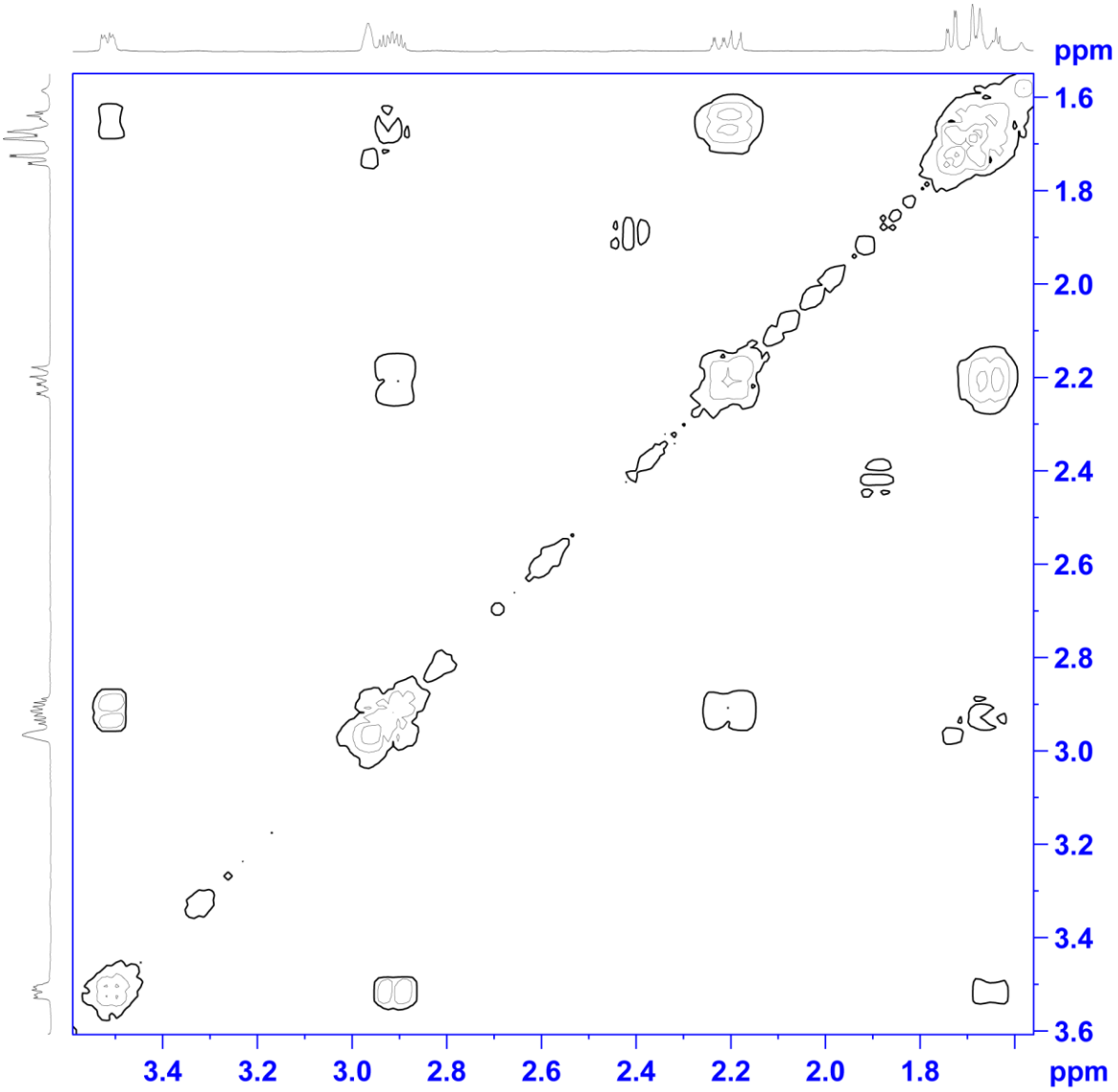

Figure S8. COSY NMR spectrum (alkyl region) for compound **10** in $CDCl_3$, recorded at 500 MHz.

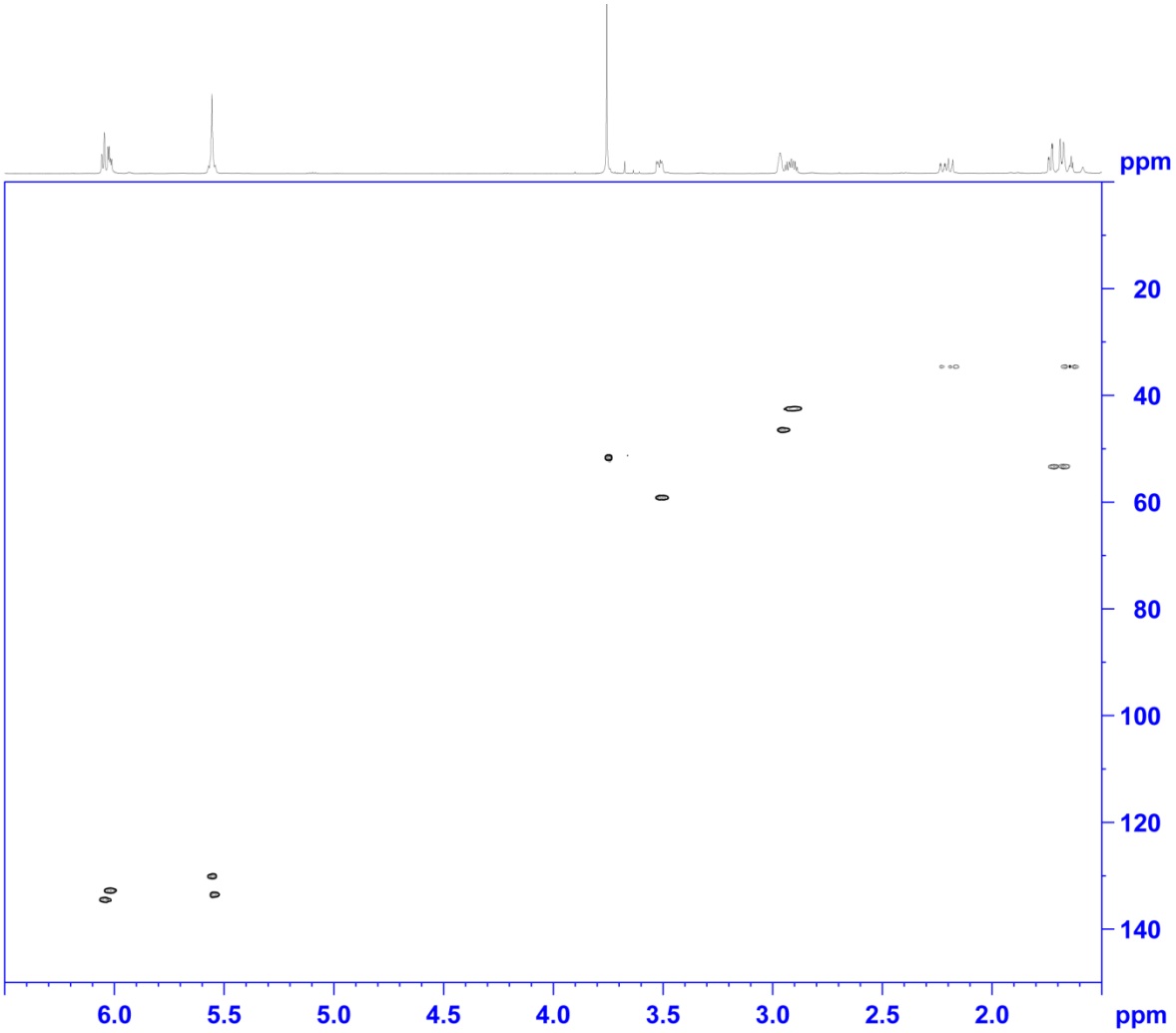

Figure S9. HSQC NMR spectrum for compound **10** in $CDCl_3$, recorded at 500 MHz x 125 MHz.

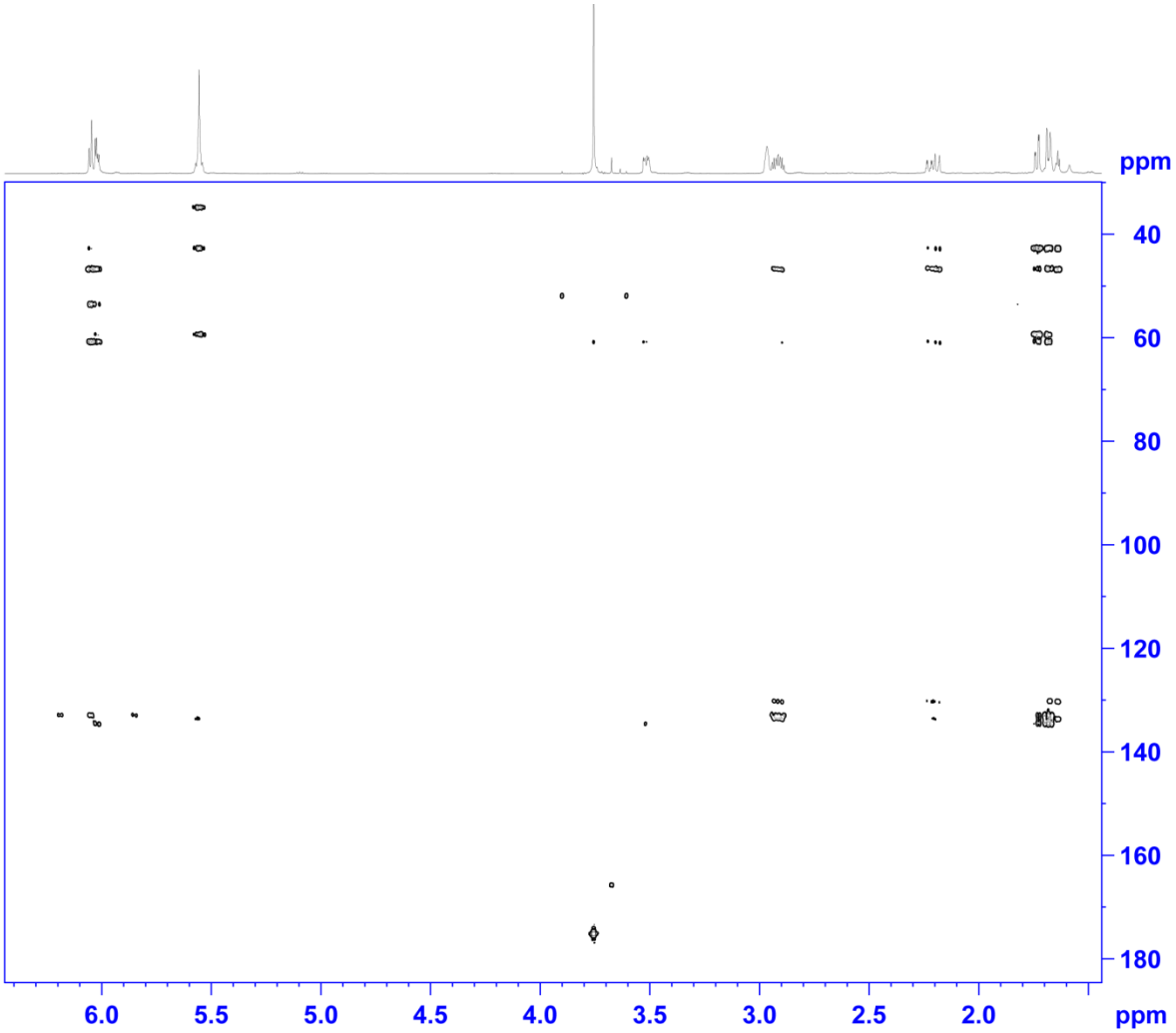

Figure S10. HMBC NMR spectrum for compound **10** in $CDCl_3$, recorded at 500 MHz x 125 MHz.

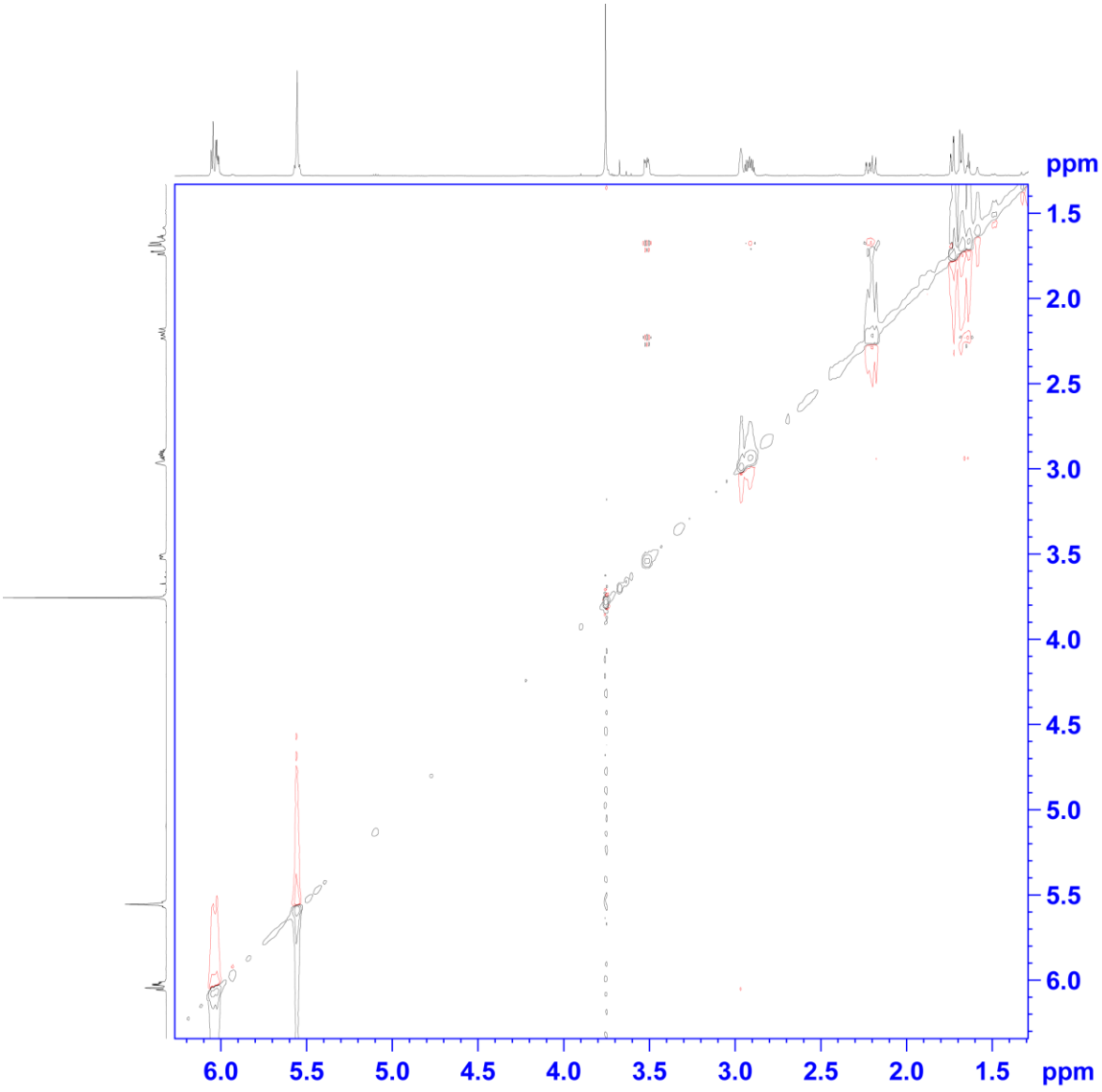

Figure S11. NOESY NMR spectrum for compound **10** in $CDCl_3$, recorded at 500 MHz.

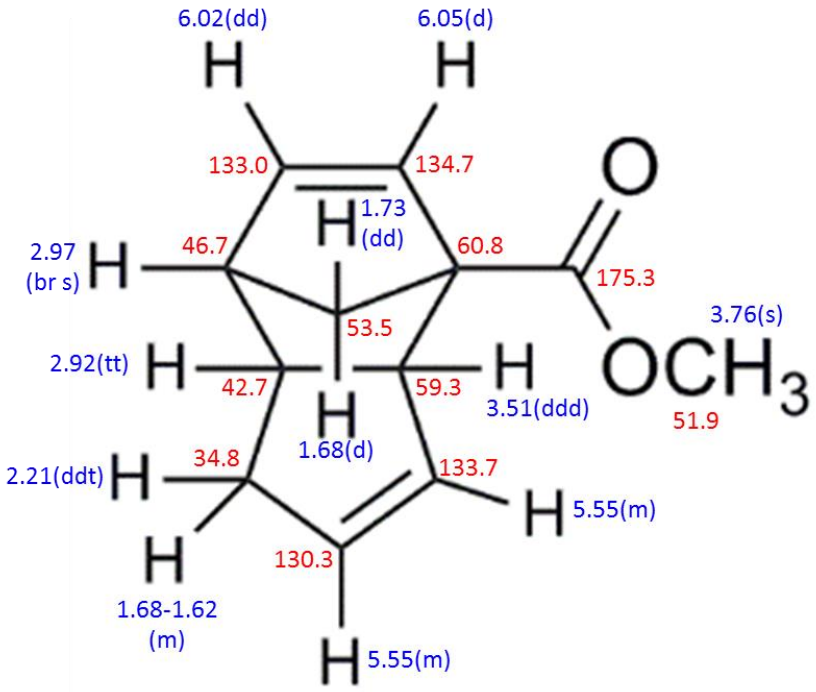

Figure S12. NMR assignments for compound **10**. Blue: ^{1}H NMR; red: ^{13}C NMR.

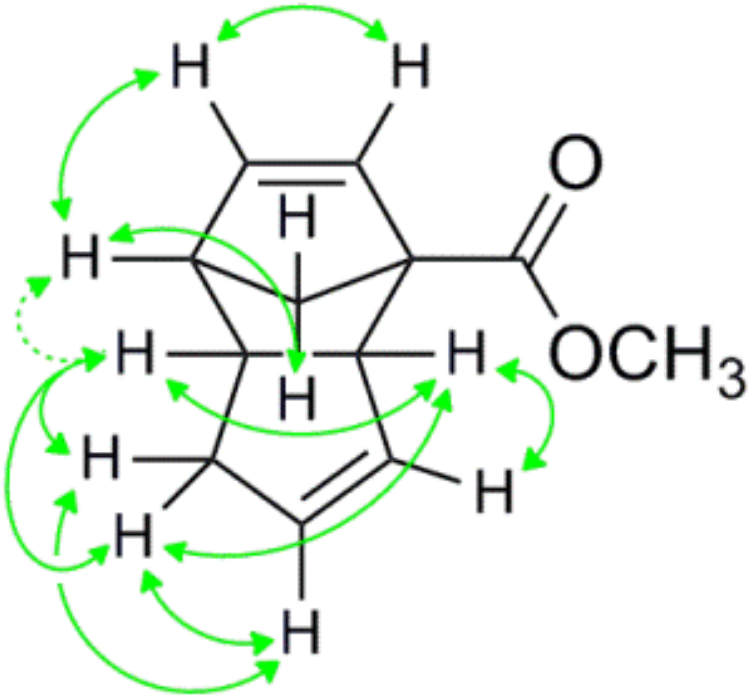

Figure S13. Significant COSY correlations for compound **10**, used to assign the structure.

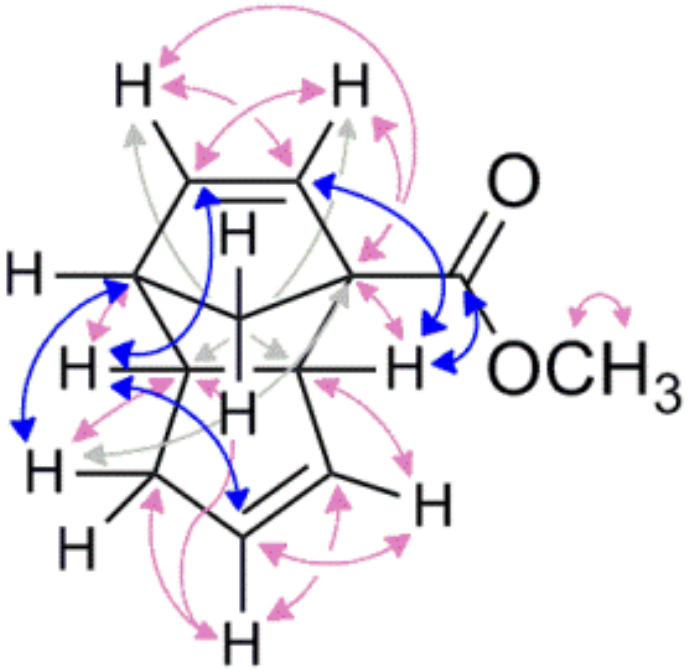

Figure S14. Significant HMBC correlations for compound **10**, used to assign the structure. Pink: confirmatory correlations establishing connectivity in the northern and southern halves of the molecule. Blue: most significant correlations establishing the relative orientation of the northern and southern fragments to one another. Grey: ^{4}J couplings present due to the constrained nature of the molecule.

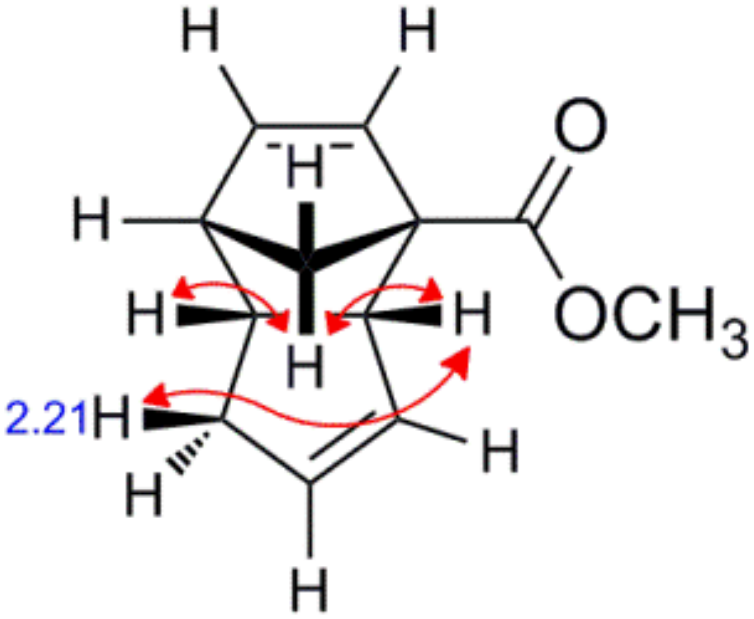

Figure S15. Significant NOE correlations for compound **10**, used to assign the structure.

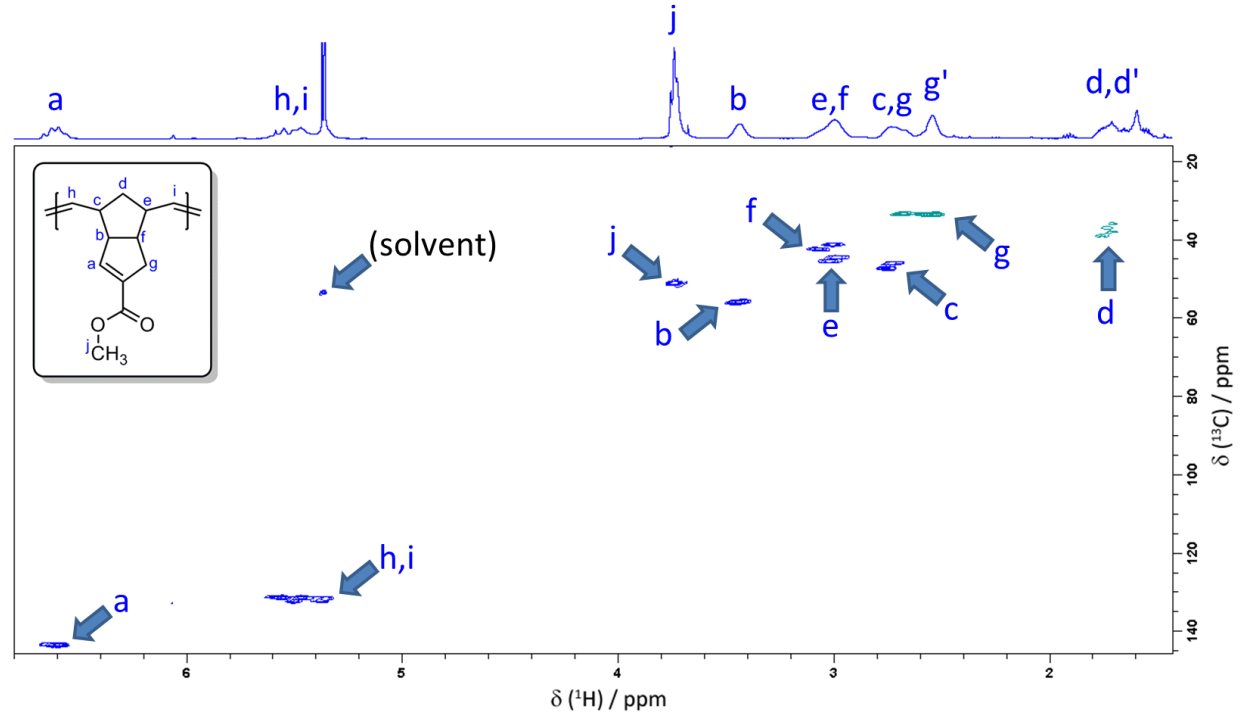

Figure S16. Full-range HSQC spectrum for linear *f*PDCPD polymer **5**, produced from column-purified monomer **4**, in CD_2Cl_2.

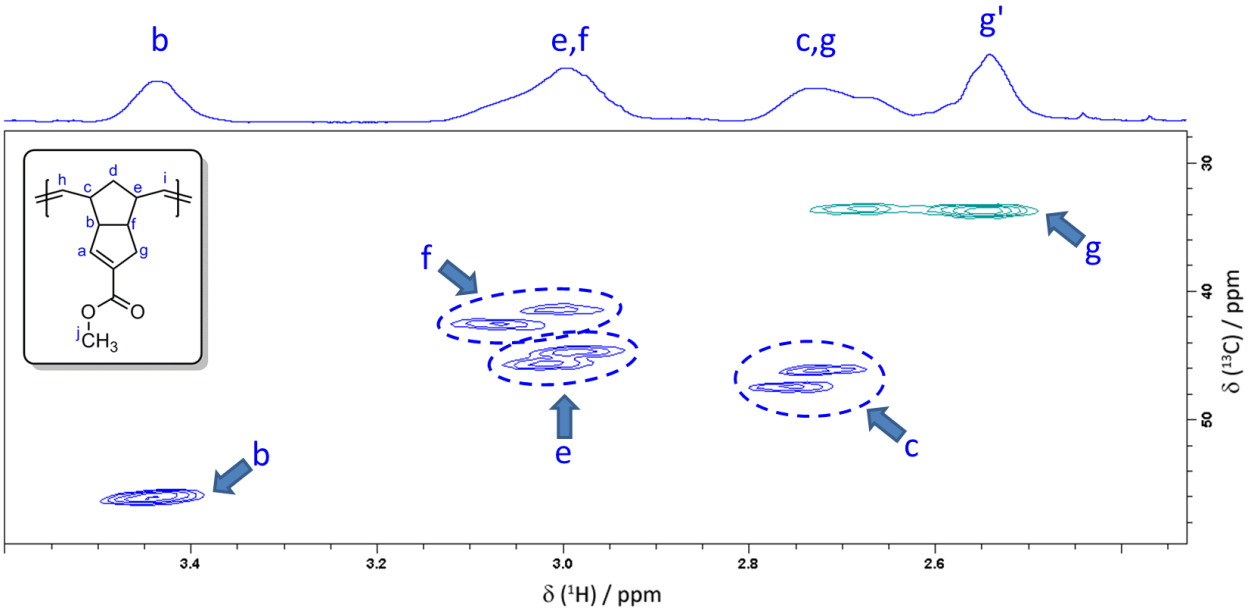

Figure S17. Close-up of HSQC spectrum for **5**, emphasizing the duplication of ^{13}C signals for some carbon atoms. This duplication could be due to the use of racemic monomer **4**, (which necessarily leads to the production of atactic polymer) but more likely is due to the possibility of both head→head and head→tail connectivity along the backbone (i.e. the primary polymer linkage could be h,c,d,e,i→h,c,d,e,i or h,c,d,e,i→i,e,d,c,h at any given backbone alkene).

Table S1. Increase in Molecular Weight with Decreasing Catalyst Concentration

catalyst loading (mol%)	integration		repeat units (n)	MW (g/mol)
	vinyl H	phenyl H		
10	1	0.1547	32.3	6147
5	1	0.1350	37.0	7044
2.5	1	0.1264	39.6	7524
1	1	< 0.08	> 60	> 10000
0.1	1	< 0.02	> 200	> 40000

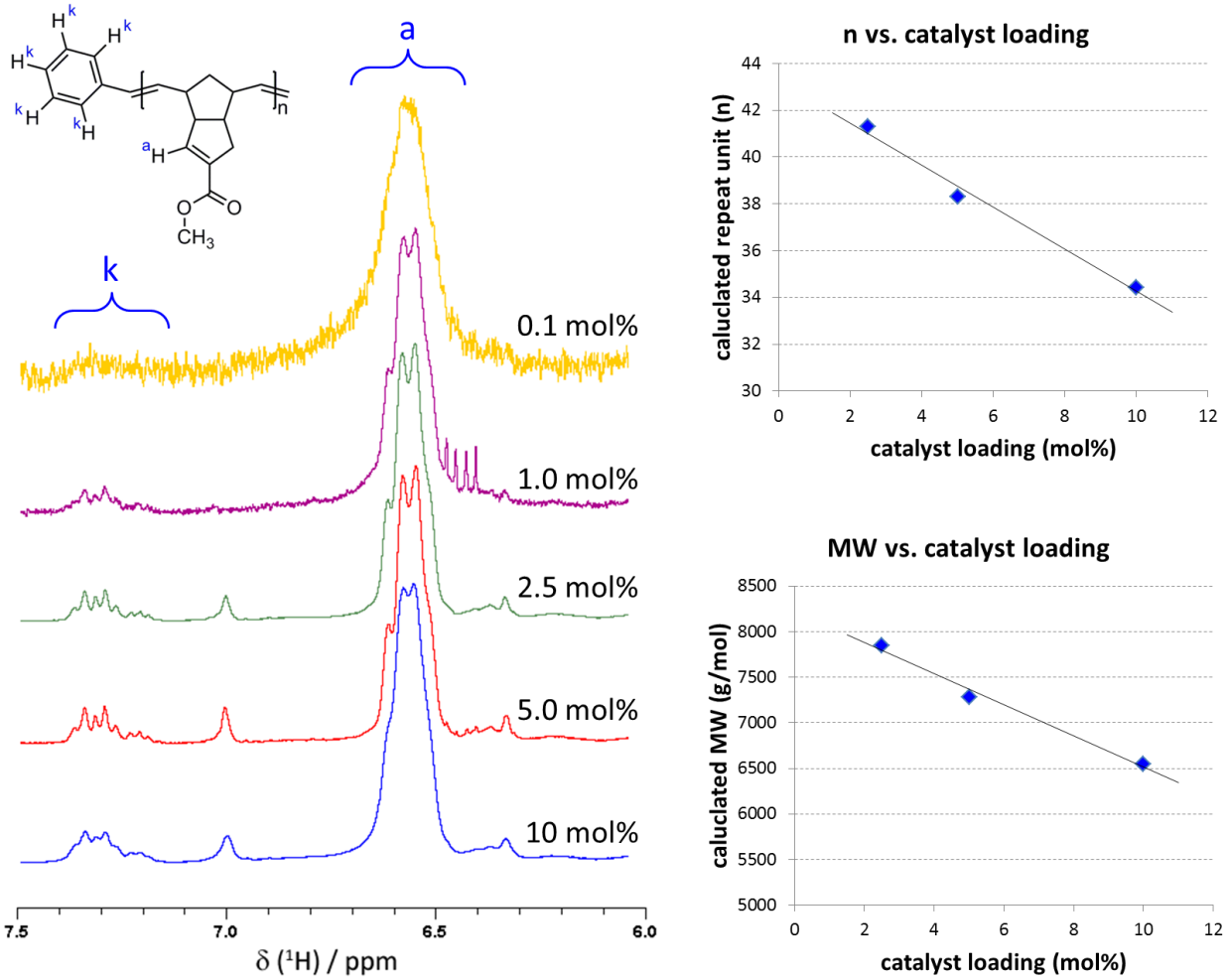

Figure S18. Increase in molecular weight with decreasing catalyst concentration.

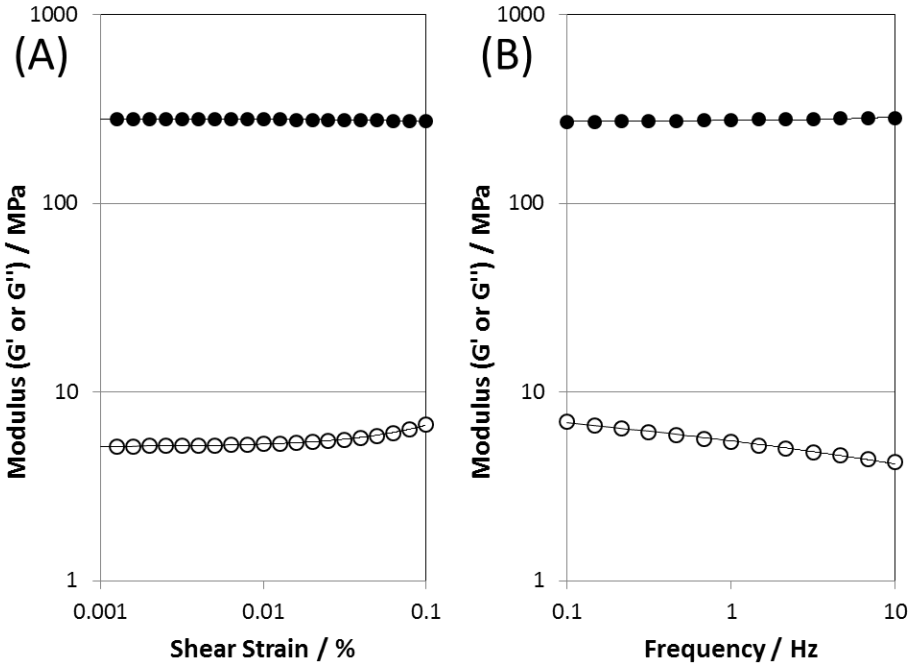

Figure S19. Amplitude and frequency sweeps for *f*PDCPD from column-purified **4**, confirming that testing parameters for the DMTA experiments were within the viscoelastic region of the material. (A) Amplitude sweep. (B) Frequency sweep. Filled data points indicate storage modulus measurements (G′); open data points indicate loss modulus (G″).